A NOVEL INHIBITORY PATHWAY LINKING PROFILIN-1 AND BREAST CANCER CELL MOTILITY

by

Yong Ho Bae

B.S. Ajou University, 1998

M.S. Rutgers University, 2005

Submitted to the Graduate Faculty of

Swanson School of Engineering in partial fulfillment

of the requirements for the degree of

Doctor of Philosophy

University of Pittsburgh

2010

UNIVERSITY OF PITTSBURGH

SWANSON SCHOOL OF ENGINEERING

This dissertation was presented

by

Yong Ho Bae

It was defended on

November 6th, 2009

and approved by

Lance Davidson, Assistant Professor, Department of Bioengineering

Cary Wu, Professor, Department of Pathology

Henry Zeringue, Assistant Professor, Department of Bioengineering

Dissertation Co-Director: Alan Wells, Professor, Department of Pathology

Dissertation Director: Partha Roy, Assistant Professor, Department of Bioengineering

A NOVEL INHIBITORY PATHWAY LINKING PROFILIN-1 AND BREAST CANCER CELL MOTILITY

Yong Ho Bae, PhD

University of Pittsburgh, 2010

Profilin-1 (Pfn1 - a ubiquitously expressed actin-binding protein) levels are significantly downregulated in various invasive adenocarcinomas including breast cancer. Although Pfn1 has been shown to be required for motility for most normal cells, breast cancer cells and normal human mammary epithelial cells exhibit a hypermotile phenotype upon Pfn1 depletion, and re-expression of Pfn1 in breast cancer cells decreases their migration. The traditionally conceived pro-migratory function of Pfn1 through its relatively well-studied interactions with actin and polyproline ligands does not provide guidance to explain this context-specific effect of Pfn1 on cell migration. The overall goal of this study is to reveal molecular mechanisms underlying the hypermotile phenotype of breast cancer cells as a result of Pfn1 downregulation. We first show that loss of Pfn1 expression increases motility of breast cancer cells by enhancing targeting of Ena(enabled)/VASP (vasodilator stimulated phosphoprotein) family of actin-binding proteins to the leading edge, a feature that is also reproducible in other cells. We further demonstrate that Ena/VASP targeting to the leading edge is mediated through the action of lamellipodin (Lpd - a membrane anchoring protein) and Pfn1 negatively regulates membrane targeting of Lpd. Limiting Lpd expression impairs motility of Pfn1-deficient breast cancer cells, thereby demonstrating loss of Pfn1 augments breast cancer cell motility through enhanced membrane recruitment of VASP/Lpd complex. Subsequent rescue experiments with various ligand-binding deficient mutants of Pfn1, we further demonstrate that Pfn1 inhibits breast cancer cell motility

mainly by its phosphoinositide interaction through negative regulation of Lpd/VASP targeting to the leading edge. Membrane targeting of Lpd in Pfn1-deficient breast cancer cells critically depends on the availability of D3-phosphorylated phosphoinositides, and consistent with this observation, we demonstrate that loss of Pfn1 expression significantly increases $PI(3,4)P_2$ presentation at the leading edge. Collectively, these findings identify a novel inhibitory mechanism of Pfn1 on breast cancer cell motility by regulating membrane availability of $PI(3,4)P_2$ and docking of Lpd, and this involves Pfn1's phosphoinositide interaction. This is in contrast to conventionally thought Pfn1's regulation of cell motility primarily through its interactions with actin and polyproline ligands.

TABLE OF CONTENTS

LIST OF FIGURES

PREFACE

I could not have finished this PhD thesis without the help and support from many people.

Most importantly, I would like to thank my PhD advisor and mentor, Dr. Partha Roy. Without his generous support, knowledgeable guidance, and optimistic encouragement, I could not have accomplished this and I cannot thank him enough.

I am also very grateful to my co-advisor, Dr. Alan Wells, for his continued support and knowledgeable instruction towards achieving my research goals throughout the years.

Also, special thanks to my thesis committee Dr. Lance Davidson, Dr. Cary Wu, and Dr. Henry Zeringue each of whom provided unique insights and directions to my research.

I would like to express my special gratitude to all the members of the Roy Lab throughout the years: Dr. Tuhin Das, Dr. Li Zou, Dr. Zhijie Ding, William Veon, Maria Jaramillo, Dave Gau, Marion Joy, and Anna DiRienzo. Their help and support has been invaluable to me.

I would like to also thank my lovely parents and mother-in-law for too many reasons to list. Last but not least, I would like to thank my dearest wife, Sun Young, for her endless love, support, and encouragement. You're the best thing that ever happened to me.

Gryson, my son, I am looking forward to meeting you soon. Love you.

ABBREVIATION

ABPs: Actin-binding proteins

AKT: A serine-threonine kinase

Arp: Actin-related protein

BSA: Bovine serum albumin

capZ: capping protein from the Z-disc of muscle

CD: Cytochalasin D

(D)PBS: (Dulbecco's) Phosphate Buffered Saline

ECM: Extracellular matrix

EGF: Epidermal growth factor

EGFR: Epidermal growth factor receptor

Ena: Enabled

EVH1: Ena-VASP homology-1

F-actin: Filamentous actin

FAK: Focal adhesion kinase

Fig: Figure

FRET: Fluorescence resonance energy transfer

GAPDH: Glyceraldehyde 3-phosphate dehydrogenase

GFP: Green fluorescent protein

GFP-PH-AKT: GFP-tagged PH domains from AKT

HMEC: Human mammary epithelial cells

HUVEC: Human vascular endothelial cells

Lpd: Lamellipodin

MDA-231: MDA-MB-231

MRL: Mig10/Rap-interacting adaptor molecule/lamellipodin

PDGF: Platelet-derived growth factor

PDGFR: Platelet-derived growth factor receptor

Pfn1: Profilin-1

PH: Pleckstrin homology

PI3K: Phosphatidylinositol 3-kinase

PI3P: Phosphatidylinositol-3-phosphate

PI(3,4)P_2: Phosphatidylinositol-3,4-bisphosphate

PI(4,5)P_2: Phosphatidylinositol-4,5-bisphosphate

PIP_3: Phosphatidylinositol-3,4,5-triphosphate

PLC: Phospholipase-C

PPI: Phosphoinositide

PLP: Proline-rich proteins

PTEN: Phosphatase and tensin homolog deleted on chromosome 10

RTKs: receptor tyrosine kinases

SDS-PAGE: Sodium dodecyl sulfate polyacrylamide gel electrophoresis

SHIP2: 5-phosphatases

siRNA: Small interfering RNA

TBST: Tris-buffered saline Tween-20

VASP: Vasodilator-stimulated phosphoprotein

VEGF: Vascular endothelial growth factor

WASP: Wiskott-Aldrich syndrome protein

1.0 INTRODUCTION

1.1 BREAST CANCER AND ITS METASTASIS

Breast cancer, the most commonly diagnosed non-skin cancer in women, is currently the second leading cause of cancer-related deaths in the United States with an estimated 40,610 deaths anticipated in the year 2009 [Welch et al., 2000; Cancer facts and Figures 2009, the American Cancer Society]. The vast majority of these cancer deaths are due to metastasis of invasive breast carcinomas to several non-adjacent organs (bone, liver, lung, and kidney) in the body resulting in cancer death. When breast cancer cells are confined within the basement membrane barrier of mammary tissue (non-invasive tumor), the patient survival rate exceeds 90% because benign tumors can be removed by surgery [Sainsbury et al., 2000]. However, once breast tumor cells metastasize, especially to the internal organs and the brain, morbidity and mortality rate increases drastically. A significant percentage of advanced breast cancer patients suffer from bone metastasis, which results in the resorption of bone, and eventually leads to osteoporosis, spinal cord compression, and fracture of long bones. As a result, the quality of life of these patients becomes severely comprised. ***Thus, elucidation of underlying cellular mechanisms of cancer metastasis and identification of molecular targets that inhibit tumor metastasis are critical for developing effective anti-metastatic therapeutics for breast cancer patients.*** Such therapeutic interventions should have a remarkable impact on not only controlling numerous

metastatic cancers but also improving the survival rate and the quality of life of both early stage and advanced breast cancer patients.

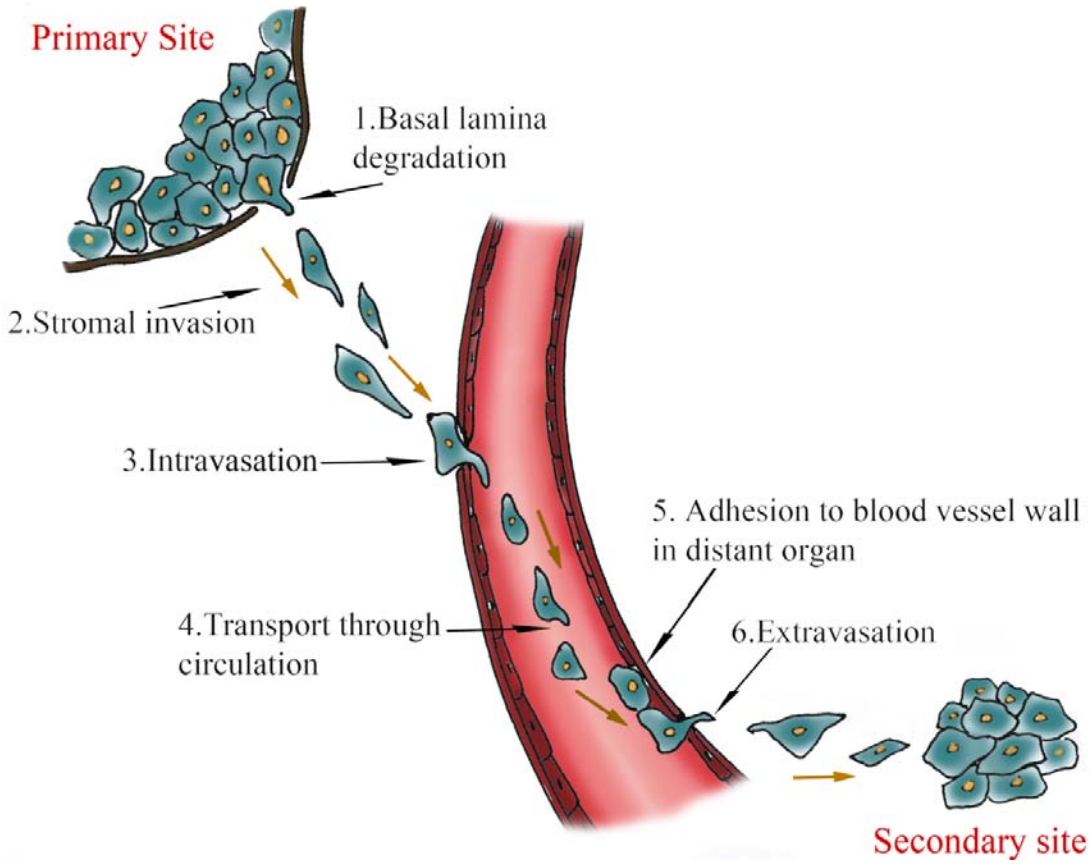

Figure 1: A schematic illustration of tumor metastasis

Chiang et al. stated that "*Metastasis is the end product of an evolutionary process in which diverse interactions between cancer cells and their microenvironment yield alterations that allow these cells to transcend their programmed behavior*" [Chiang et al., 2008]. Metastatic breast cancer cells from the primary tumor at the luminal epithelial lineage of terminal duct lobular units of the breast initiate by genetic alterations, thereby, these tumor cells are able to acquire new functions for metastatic potentials which facilitate their propagation to distant regions [Petersen et al., 2001; Chiang et al., 2008]. Distant metastasis of tumor is a multi-stage

process (schematically represented in Fig 1) and involves numerous signaling pathways. Metastasis of breast cancer is critically dependent on neovascularization (angiogenesis) in the tumor which provides a route for distant metastasis [Schneider et al., 2005]. To metastasize, aggressive malignant cells, which have lost the ability to adhere with their adjacent cells, dissociate from the localized primary tumor site and penetrate the surrounding connective tissue by breaking the dense basement membrane **[BASAL LAMINA DEGRADATION AND INVASION]**. Next, these disseminated tumor cells secrete factors that promote vascular endothelial cell contraction which causes retraction of the cell-cell junctions and impairs endothelial cell barrier function by creating gaps between endothelial cells so that cells can enter blood microvessels (hematogenous dissemination) or the lymphatic routes (lymphatic dissemination) **[INTRAVASATION]**. These cancer cells are transported through circulation to distant secondary sites where they may be trapped and subsequently leave the vasculature to enter the secondary target site **[EXTRAVASATION]**. Then, tumor cells invade to normal surrounding tissue and form dormant micrometastases. Eventually some of micrometastases proliferate and form solid macroscopic metastases in the secondary target organ [Enger et al., 2000; Wyckoff et al., 2000; Lambrechts et al., 2004]. One of the essential steps of the tumor metastasis to other sites is cell invasion to adjacent connective matrix, which requires active cell migration. At the molecular level, cancer cell migration is correlated with deregulated actin cytoskeleton.

1.2 DEREGULATION OF ACTIN CYTOSKELETON SIGNALING IN CANCER CELL MIGRATION

Cell motility (schematically represented in Figure 2), a fundamental aspect of cancer invasion and metastasis, requires an asymmetry of biophysical and mechanical cell processes in a cyclic nature [Yamaguchi et al., 2005; Feldner et al., 2002; Lauffenburger et al., 1996]. Thus, dissecting molecular mechanisms of cell migration is an indispensable first step in understanding the behavior of cancer cells, thereby, preventing or limiting the invasion and metastasis of cancer.

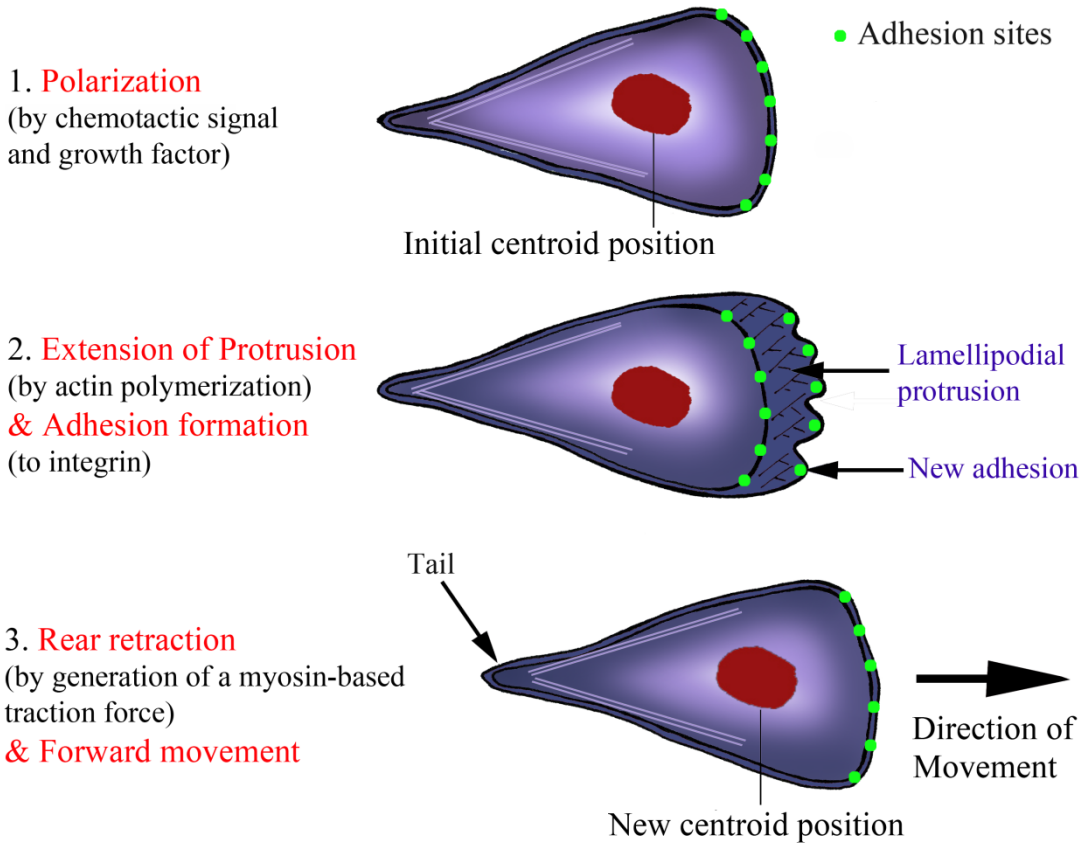

Figure 2: A schematic illustration of cell migration [modified from (Ridley et al., 2003)]

In order for cell migration to occur, actin cytoskeletal reorganization in cells is a prerequisite to protrude their leading edge and to generate contractility that directed to net cell movement. Actin dynamics in motile cells is regulated by a large number of actin-binding proteins (ABPs) including those engaged in G-actin sequestering (thymosin β4), nucleation of actin filaments (Arp2/3, WASP, formin), elongation of actin filaments (Ena/VASP, formin), nucleotide exchange on G-actin and shuttling of G-actin to barbed ends of growing actin filaments (profilin), capping (capZ), severing/depolymerization (actin depolymerizing factor (ADF)/cofilin, gelsolin), and cross-linking/stabilization (filamin, fascin, cortactin) [Pollard et al., 2003; Roy et al., 2008]. Disruption of actin cytoskeleton is a characteristic of malignant cells, and this correlates with altered expression and/or activity of wide-range of ABPs [Roy et al., 2008; Clark et al., 2000; Wang et al., 1996].

To migrate/invade to connective tissues and infiltrate into blood vessels, cells are initially required to polarize by migration-promoting molecules or microenvironments that include motogenic agents (growth factors such as EGF (epidermal), PDGF (platelet-derived), and VEGF (vascular endothelial)), chemokines (chemotactic cytokines that include four subfamilies; C, CC, CXC, and CX3C, (C: a cysteine; X: any amino-acid residue) [Rottman et al., 1999]), cytokines (secreted molecules that signal through G-protein-linked receptors), and extracellular matrix (ECM) [Huttenlocher et al., 2005]. In response to migration stimuli, cells subsequently extend their lamellipodia (flat, sheet-like membrane network of actin filaments) or filopodia (thin, spike-like cytoplasmic projection) for leading membrane protrusions in a given direction due to enhanced actin polymerization at the cell's front. Once the migration path is defined, the protrusive machinery for facilitating movement assembles with regard to the directional migration. Membrane modifying enzymes that are associated with the inner membrane surface

(example: phospholipase C-γ (PLCγ) and phosphatidylinositol 3-kinase (PI3K)) are activated at the downstream of various receptor tyrosine kinases (RTKs) such as a induce actin cytoskeletal reorganizations by altering membrane docking phospholipid-binding ABPs (profilin, cofilin, capping protein, and gelsolin) [Roy et al., 2008; Rheenen et al, 2007]. These ABPs in turn regulate actin meshwork at the cell's leading edge by modulating actin turnover [Pollard et al, 2003; Chen et al., 1996; Janmey et al., 1994; Allen et al., 2003; Goldschmidt-Clermont et al., 1991; Bae et al., 2006].

Next, cells create new focal adhesions to ligands (collagen, fibronectin, laminin, and fibrinogen) in the ECM (the basal lamina, connecting fibers, connective tissue) or to molecules (cadherins) on the surface of adjacent cells through the binding of transmembrane receptors (integrins; a family of αβ heterodimers) which are linked with intracellular molecules (actinin, talin, vinculin, and filamin) that bind intracellular actin filaments inside. All of this acts to stabilize the dominant protruding lamellipodia at the leading edge of the cell membrane [Ridley et al., 2003; Sheetz et al., 1999; Roy et al., 2008]. In addition to ECM components, integrins attach to a cytoplasmic complex such as focal adhesion kinases (FAK) and Src family kinases to mediate adhesion to the actin cytoskeleton.

The cell-substratum attachment is followed by de-adhesion and retraction at the rear end of the cell, but the leading edge stays attached to the ECM. These final processes require myosin II (an actin-based motor protein in eukaryotic non-muscle cells)-based contraction of actin filaments which generate a sufficient amount of force/tension, to provide forward movement of the cell [Sheetz et al., 1999]. Movement over an extended distance occurs through many repetitions of this cycle in a directionally-persistent manner. The forward protrusion by actin polymerization establishes the directionality and protrusive force of the cell, even in the absence

of a signaling gradient [Sheetz et al., 1999; Roy et al., 2008]. Overall, acquisition of the invasive phenotype by malignant cells is correlated with active reorganization of the actin cytoskeleton by deregulated expression of various ABPs [Feldner et al., 2002; Pawlak et al., 1999]. The malignant phenotype of tumor cells often can be reversed by experimental restoration of ABP expression, signifying that misregulation of ABPs could contribute directly to malignancy [Nikolopoulos et al., 2000; Tanaka et al., 1995]. Consistent with these findings, reduced expression of profilin-1 (Pfn1- an important actin regulatory protein) has been reported in various invasive adenocarcinomas including breast cancer cell. Whether there is any fundamental link between reduced Pfn1 expression and increased aggressiveness of various adenocarcinoma remains to be determined.

1.3 PROFILIN-1 BIOCHEMISTRY

Presently, four different mammalian profilin genes have been identified: Pfn1 (a member of profilin that is ubiquitously expressed in all cell types except skeleton muscle tissue [Witke et al., 1998]), Pfn2 (has two splice variants [Pfn2a and Pfn2b] which are mainly expressed in the cells of neural tissues [Witke et al., 1998; Giesemann et al., 1999]), Pfn3 (expression restricted to t kidney and testis) and Pfn4 (expression limited to testis) [Lambrechts et al., 2000; Hu et al., 2001; Obermann et al., 2005]). From here, only Pfn1 will be reviewed and discussed in my thesis because of its implications in cancer. Pfn1 is capable of interacting mainly with three classes of ligands including actin monomers, many proline-rich proteins and various polyphosphoinositides [Fedorov et al., 1994; Metzler et al., 1994; Chaudhary et al., 1998; Mahoney et al., 1999]. Pfn1 was initially reported as a G-actin sequestering protein [Karlsson et al., 1977].

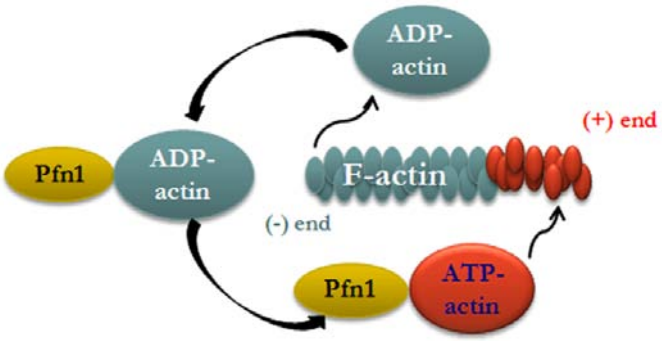

Figure 3: Pfn1's role in actin polymerization [modified from (Witke et al., 2004)]

However, subsequent studies revealed that ***one of the major roles of Pfn1 is to promote actin polymerization in cells*** (schematically represented in Figure 3) by 1) accelerating the nucleotide exchange rate of ADP-to-ATP on G-actin, and 2) transporting ATP-G-actin to the free and fast-growing barbed ends of actin filaments [Karlsson et al., 1977; Pantaloni et al., 1993; Kang et al., 1999; Schluter et al., 1997; Bubb et al., 2003; Goldschmidt-Clermont et al., 1990; Witke et al., 2004].

Besides actin, Pfn1 also associates with a number of proline-rich proteins (PLP) that control actin assembly by promoting either nucleation and/or elongation of actin filaments at the leading edge, including proteins belonging to the Ena (enabled)/VASP (vasodilator stimulated phosphoprotein) [Ferron et al., 2007], N-WASP (Neural Wiskott Aldrich syndrome protein; the ubiquitously expressed member of WASP [Suetsugu et al., 1998]), WAVE (WASP family verprolin-homologous protein [Miki et al., 1998]), and diaphanous [Miki et al., 1998; Watanabe et al., 1999] protein families. Limiting Pfn1 expression resulting in slightly decreased total F-actin level in various cells is consistent with this actin-regulatory function of Pfn1 [Ding et al., 2006; Zou et al., 2007; Ding et al., 2009] . It has been proposed that ***these extracellularly-activated PLP may potentially act as molecular scaffolds to spatially recruit the Pfn1-actin***

complex to sites of actin assembly at the leading edge during active cell migration [Holt et al., 2001].

In addition to actin and PLP ligands (proteins containing polyproline domains), Pfn1 also binds to plasma membrane most likely through its interactions with various phosphoinositides (PPIs) including phosphatidylinositol-4,5-bisphosphate ($PI(4,5)P_2$), phosphatidylinositol-3,4-bisphosphate ($PI(3,4)P_2$; generated by dephosphorylation of PIP_3 by PI-5-phosphatase) and phosphatidylinositol-3,4,5-triphosphate (PIP_3; generated by the phosphorylation of $PI(4,5)P_2$ by PI3K) [Lu et al., 1996], potentiating it as a mediator between the cell membrane and cytoskeleton [Machesky et al., 1993]. $PI(3,4)P_2$ and PIP_3 are generated by activation of phosphoinositide 3-kinase (PI3K) and have a greater binding affinity to profilin than $PI(4,5)P_2$ [Lu et al., 1996]. Mammalian Pfn1 has two PPI binding regions, one largely overlapping with its actin-binding site and the other partially overlapping with its PLP binding site. It has been suggested that Pfn1 binding to PPI mostly inhibits its interaction with actin [Skare et al., 2002; Lassing et al., 1985].

Among the different ligand-binding abilities of Pfn1, the actin and PLPs interactions have been most heavily investigated in the literature, mainly in the context of cytoskeletal regulation. However, very little known about Pfn1's interaction with membrane PPIs which has been almost exclusively investigated in vitro using pure protein-phospholipid mixture [Goldschmidt-Clermont et al., 1990] and therefore, physiological and pathological implications of Pfn1's interaction with membrane PPIs has not been explored in vivo. Signaling events downstream of PPIs play a major role in cell motility. However, whether Pfn1's interactions with various membrane phospholipids have any modulatory function on cell migration has not been investigated in depth. Although it remains to be investigated, based on Pfn1's ability to inhibit

PLC-mediated PI(4,5)P_2 hydrolysis in vitro [Goldschmidt-Clermont et al., 1990] and a recent study by our group directly showing for the first time that significant suppression of PIP_3 generation in Pfn1-overexpressed breast cancer cells [Das et al., 2009], one could envision that Pfn1 may regulate membrane PPI metabolism by posing steric hindrance to some docking proteins and metabolic enzymes of PPIs through competition for lipid binding and in turn affect cell motility. Since these in vitro (using purified proteins and lipid micelles) and in vivo (using Pfn1 overexpression system in breast cancer cells) studies could not thoroughly show Pfn1's interaction with specific PPI cellular processes in detail, ***Pfn1's role in PPI metabolism and its functional significance needs to be revisited in a cellular context***.

1.4 PROFILIN-1'S ROLE IN NORMAL AND CANCER CELL MIGRATION

Numerous previous studies identify Pfn1 as an important actin-binding protein in the overall balance of actin polymerization in cells. However, its exact role in cell migration has not been well understood until recently. The first direct evidence of Pfn1's role in cell migration is from a study on *Dictyostelium* amebae mutants deficient in both Pfn1 and Pfn2, which demonstrated considerably impaired cytokinesis and cell motility [Haugwitz et al., 1994]. In addition, *Drosophila* harboring Pfn1-mutants exhibited developmental defects [Verheyen et al., 1994]. Profilin is necessary for motor axon outgrowth in the *Drosophila* Embryo [Wills et al., 1999] and *C. elegans* requires Pfn1 function for embryogenesis [Velarde et al., 2007]. Dependence of actin-driven intracellular propulsion of bacterial pathogens on Pfn1 (Loisel et al., 1999; Mimuro et al., 2000), impaired membrane protrusion of HUVECs (Human vascular endothelial cells) as a result

of Pfn1 downregulation [Ding et al., 2006], and very recently, induction of lamellipodia by Pfn1 in a growth-factor insensitive mechanism [Syriani et al., 2008] all point to a key role of Pfn1's function in driving membrane protrusion during most normal cell migration. In addition, studies by our group showed that both actin and PLP interactions of Pfn1 contribute to membrane protrusion and overall cell migration at least for vascular endothelial cell lines [Ding et al., 2006; Ding et al., 2009]. Collectively, these experimental evidences suggest that Pfn1 is a critical prerequisite molecule for normal cell migration and development.

Interestingly however, significant reduction of Pfn1 expression has been shown in various types of highly invasive adenocarcinoma (a cancer originating in glandular epithelial tissue including breast, pancreatic, hepatic, and gastric) when compared to their non-tumorigenic counterparts [Gronborg et al., 2006; Janke et al., 2000; Wu et al., 2006; Oien et al., 2003]. A moderate overexpression of Pfn1 in CAL51 (epithelial, human breast carcinoma) and MDA-231 breast cancer cell lines significantly inhibits its tumorigenic potential in nude mice [Janke et al., 2000; Wittenmayer et al., 2004; Roy et al., 2004; Zou et al., 2007] suggesting that Pfn1 could be a tumor-suppressor protein as well. These experimental data are also consistent with immunohistological findings of graded Pfn1 downregulation with increased cancer grade [Janke et al., 2000]. Similarly, retinoic acid-induced suppression of hepatocarcinoma cell migration can be reversed by downregulating Pfn1 [Wu et al., 2006]. Previous studies from our lab show that loss of Pfn1 expression results in increased motility of both normal human mammary epithelial cells (HMEC) and MDA-231 breast cancer cells [Zou et al., 2007]. Conversely, restoring Pfn1 levels by overexpression significantly impairs the aggressive phenotype of breast cancer cells (Roy et al., 2004; Zou et al., 2007). Collectively, these findings raises a possibility that Pfn1 downregulation could lead to increased breast cancer invasion and metastasis in vivo. However,

given the plethora of evidence demonstrating importance of Pfn1 in driving actin polymerization at the leading edge and hence playing a critical role in cell migration, the existing literature fails to explain how loss of Pfn1 expression might contribute to enhanced motility of breast cancer cells at a mechanistic level. ***The overall goal of my research is to elucidate molecular mechanisms underlying the hypermotile phenotype of breast cancer cells as a result of Pfn1 downregulation.***

2.0 HYPOTHESIS AND SPECIFIC AIMS

Given the generally considered pro-migratory role of Pfn1 mediated primarily through its actin and polyproline interactions, the existing studies cannot intuitively elucidate how loss of Pfn1 expression augments carcinoma cell motility. My preliminary studies demonstrate that loss of Pfn1 expression enhances lamellipodial targeting of Ena/VASP proteins in several different cell lines including HUVEC, HMEC and MDA-231cells [Bae et al., 2009]. It has been recently shown that fish keratocytes (an extremely fast migrating epithelial cell type) migrate faster and in a smooth, gliding fashion when Ena/VASP family proteins are enriched at their leading edge [Lacayo et al., 2007]. Leading edge targeting of Ena/VASP has also been shown to result in faster membrane protrusion [Bear et al., 2002]. Recent studies further show that Ena/VASP proteins play a major role in chemotactic invasion of breast cancer cells [Philippar et al., 2008]. Lamellipodin (Lpd), a member of MRL (Mig10/ Rap1-interacting adaptor molecule / lamellipodin) family of actin-binding proteins which contain a pH domain with binding specificity $PI(3,4)P_2$, has been identified as one of the potential linker for targeting Ena/VASP close to the plasma membrane at the leading edge. Herein, ***I postulate that limiting Pfn1 expression in breast cancer cells enhances D3-phosphoinositide (such as $PI(3,4)P_2$) presentation at the leading edge of migrating cells, allows increased access of lamellipodin to the plasma membrane and creates a hypermotile phenotype***.

To test the overall hypothesis, I proposed the following aims:

Specific Aim1: ***To determine whether VASP plays a role in the hypermotile response of breast cancer cells induced by loss of Profilin-1 expression.***

Specific Aim2: ***To e**xamine whether Profilin-1 inhibits breast cancer cell motility by regulating D3-phosphoinositide availability for lamellipodin targeting to the membrane.***

3.0 MATERIALS AND METHODS

3.1 ANTIBODIES AND REAGENTS

Polyclonal Pfn1 and GAPDH antibodies were purchased from Cytoskeleton (Denver, CO- in some experiments, a different polyclonal Pfn1 antibody that was kindly provided by Dr. Sally Zigmond of the University of Pennsylvania was used) and Abd Serotec (Raleigh, NC), respectively. Polyclonal GFP and monoclonal VASP antibodies was obtained from Pharmingen (San Diego, CA). Polyclonal Lpd antibody was purchased from Santa Cruz Biotechnology (Santa Cruz, CA- in some experiments, a different polyclonal Lpd antibody that was supplied by Dr. Frank Gertler of the Massachusetts Institute of Technology was used). Polyclonal cofilin antibody was purchased from Abcam (Cambridge, MA). Monoclonal $PI(3,4)P_2$ antibody was obtained from Echelon Biosciences (Salt Lake City, Utah). Polyclonal EGFR, AKT and phospho-AKT (S473) antibodies are products of Cell Signaling Technology (Danver, MA). Polyclonal PDGFR-β antibody was kindly provided by Dr. Paul Monga (University of Pittsburgh). Monoclonal phosphotyrosine and phospho-EGFR (Y1173) antibodies were obtained from Upstate Biotechnology (Billerica, Massachusetts). All cell culture reagents are products of Invitrogen (Carlsbad, CA). PI3-kinase inhibitor LY294002 was purchased from Calbiochem (Carlsbad, CA). Cytochalasin-D was purchased from Cytoskeleton, Inc. (Denver, CO). Plasmids encoding Ena/VASP sequestration (FP4-mito) and corresponding control (AP4-mito) constructs

were generated in Dr. Gertler's laboratory as previously described [Bear et al., 2000; Bear et al., 2002] and subsequently subcloned in mCherry vector. Expression vectors for GFP-PTEN and GFP-PH-AKT were generously provided by Drs. Pier Pandolfi (Beth Israel Deaconess Medical Center) and Tamas Balla (National Institute of Health), respectively. The sequences of Control and Pfn1 siRNAs have been previously described [Bae et al., 2009]. A pool of Lpd siRNAs was obtained from Santa Cruz Biotechnology (Santa Cruz, CA).

3.2 CELL CULTURE AND TRANSFECTION

MDA-231 breast cancer cells were cultured in EMEM media (supplemented with 10% FBS, sodium pyruvate and antibiotics (Invitrogen - Carlsbad, CA). HMEC and HUVEC (source: Cambrex, Walkersville, MD) were cultured in a complete growth media supplied by the manufacturer. All Pfn1 constructs were generated by site-directed mutagenesis and rendered Pfn1-siRNA-resistant by introducing silent mutation in the siRNA targeting region without changing their peptide encoding (targeting region of Pfn1-siRNA has been previously described [Bae et al., 2009]). MDA-231 cells stably transfected with various Pfn1 constructs (using lipofectamine 2000 reagent (Invitrogen- Carlsbad, CA) were maintained in complete growth media supplemented with 500 μg/ml G418. The working concentration for various siRNAs were: Pfn1 (50 nM for MDA-231, 100 nM for HUVEC and HMEC) and Lpd (100 nM). SiRNA transfection was performed using reagents commercially available from Dharmacon (Lafayette, CO) according to the manufacturer's instruction and all silencing-based experiments were performed 72 hours after transfection.

3.3 IMMUNOSTAINING

Cells were washed with DPBS, fixed with 3.7% formaldehyde for 15 minutes, permeabilized with 0.5% Triton X-100 for 15 minutes and then blocked with 10% goat-serum for 1 hour at room temperature. After incubating with the primary antibodies (VASP and/or Lpd at 1:100 dilution; Pfn1 antibody at 1:50 dilution) for 1 hour at room temperature, cells were washed two times with DPBS containing 0.02% tween and 2 times with DPBS and then incubated with secondary antibodies (source: Jackson Immunoresearch, West Grove, PA) with or without alexa-488 phalloidin (Invitrogen) for an additional hour at room temperature. Stained cells were washed two times with DPBS containing 0.02% tween, two times with DPBS, and then once with distilled water before mounting on slides for imaging using a 60X oil-immersion objective on an Olympus IX71 inverted microscope. Quantitative fluorescence analyses of images were performed by Metamorph or ImageJ. Specifically, for VASP and Lpd quantification at the leading edge, images were first background subtracted (the average intensity of cell-free area on the coverslips was used for background correction), and the average fluorescence intensity at the very leading edge (identified by phalloidin counterstaining) was then calculated based on 15-20 line scan measurements across the lamellipodia.

3.4 $PI(3,4)P_2$ IMMUNOSTAINING AND QUANTIFICATION

Cells were serum-starved for 30-40 hours and then stimulated with either EGF or PDGF (working concentration -100 ng/ml) for 30 minutes before performing $PI(3,4)P_2$ immunostaining according to a previously described protocol [Yip et al., 2008]. Briefly, cells were fixed and

permeabilized with 3.7% paraformaldehyde and 0.1% glutaraldehyde in 0.15 mg/ml saponin solution for 1 hour at 37°C. Cells were incubated with anti-PI(3,4)P_2 antibody diluted in PBS-5% BSA (1:200) for 1 hour, after which they were washed 4 times with PBS, incubated with rhodamine-conjugated secondary antibody for 45 minutes and washed again 4 times in PBS before mounting for microscopy. Images were acquired with a 60X objective on an Olympus Fluoview 1000 inverted confocal microscope and were background subtracted before quantitative fluorescence intensity analyses. For PI(3,4)P_2 quantification at the leading edge, the average fluorescence intensity was then be quantitated based on 10 line scan measurements across the lamellipodia. These values were then normalized with respect to the average fluorescence value calculated for control-siRNA treated cells in serum-starved condition.

3.5 PROTEIN EXTRACTION AND IMMUNOBLOTTING

Total cell lysate (TCL) was prepared by extracting cells with warm 1X sample buffer or modified RIPA buffer (50 mM Tris-HCl - pH 7.5, 150 mM NaCl, 1% NP-40, 0.25% sodium deoxycholate, 0.3% SDS, 2 mM EDTA) supplemented with 50mM NaF, 1mM sodium pervanadate, and protease inhibitors (10 µg/ml of leupeptin, aprotinin, pepstatin and 1 mM phenylmethylsulfonyl fluoride). For sub-cellular fractionation analyses of GFP-Pfn1, cells were washed twice with cold PBS and extracted with 0.5% saponin in hypotonic buffer (10mM HEPES, pH7.9, 10mM KCl, 0.1mM EDTA, 1mM DTE with protease and phosphatase inhibitors) for 10 minutes to obtain the cytosolic fraction. Further extraction with 1% Triton-X100 in hypotonic buffer for 15 min followed by clarification of the extract at 18000g for 15 minutes yielded the membrane fraction. For immunoblotting, protein concentration was first

determined by a coomassie-based protein assay kit. Proteins separated with SDS-PAGE were transferred onto a nitrocellulose membrane. After blocking the membrane with the appropriate blocking solution in TBST for 1 hour at room temperature, immunoblotting was performed by overnight incubation at 4℃ with the appropriate primary antibodies. The antibodies were used at the following concentrations: GAPDH (1:2000), Pfn1 (1:500), VASP (1:1000), GFP (1:1000), cofilin (1:3000), Lpd (1:1000), AKT (1:500), phospho-AKT (1:500), EGFR (1:1000), phospho-EGFR (1:200), PDGFR-β (1:200), and pY-PDGFR (1:1000). After washing 5 times with TBST, the blot was incubated with the appropriate secondary antibody, washed 4 times with TBST and finally once with distilled H_2O before performing chemiluminescence for visualizing protein bands.

3.6 FLUORESCENCE BASED F-ACTIN QUANTIFICATION

Cellular level of F-actin was quantitated using a rhodamine-phalloidin binding assay as previously described [Diakonova et al., 2002]. Cells ($3.6x10^5$) were seeded in 2-3 replicates in the wells of a collagen-coated 6-well plate. After 4 hours of incubation, cells were fixed with 3.7% formaldehyde for 15 min, permeabilized with 0.5% Triton X-100, and then co-stained with rhodamine-phalloidin and DAPI (for normalization of cell number) for 1 hour at room temperature. After washing cells three times with PBS, rhodamine-phalloidin was extracted with 500 µl of methanol for 1 hour in the dark; cells were finally extracted with 300 µl of lysis buffer. Fluorescence readings of rhodamine (excitation 540 nm, emission 575 nm) and DAPI (excitation 358 nm, emission 461 nm) were acquired using a spectrofluorometer and the ratio of rhodamine to DAPI fluorescence was calculated.

3.7 TIME-LAPSE CELL MOTILITY AND KYMOGRAPH ASSAYS

Cells, sparsely plated overnight on collagen-coated 35-mm culture dish, were imaged for 2-3 h at a 1-min time-interval between the successive image frames. For all time-lapse recordings, proper environmental conditions (37°C/pH 7.4) were maintained by placing the culture dish in a microincubator. Cell trajectory was constructed by frame-by-frame analyses of the centroid positions (x, y) of cell-nuclei (assumed to be the representations of cell-bodies). The change in the direction of centroid movement between successive image frames (i-1, i, i+1) was calculated as $\Delta\theta_i = \Delta\theta_{i,\, i+1} - \Delta\theta_{i,\, i-1}$ ($\Delta\theta_{i,\, i+1} = \cos^{-1}(x_{i+1} - x_i)/\text{sqrt}\ ((x_{i+1} - x_i)^2) + ((y_{i+1} - y_i)^2)$) and from these values, the standard deviation of $\Delta\theta$ was computed. For kymography, additional time-lapse movies were recorded for 10-20 min at a 5-sec time-interval. Kymographs marking the beginning to the end of protrusion were constructed based on 1-pixel wide (0.3 μm) lines drawn at multiple locations (3-4) across the protruding membrane. Membrane fluctuation <4 pixels (1.2 μm) was disregraded for quantitative analyses. All images were acquired and analyzed using Metamorph and NIH ImageJ softwares, respectively.

3.8 STATISTICS AND DATA REPRESENTATION

All statistical tests were performed with ANOVA followed by Neuman-Keuls post-hoc test for multiple comparisons whenever applicable, and a p value less than 0.05 was considered to be

statistically significant. In most cases, experimental data were represented as box and whisker plots where dot represents the mean, middle lines of box indicates median, top of the box indicates 75^{th} percentile, bottom of the box measures 25^{th} percentile and the two whiskers indicate the 10^{th} and 90^{th} percentiles, respectively.

4.0 ROLE OF ENA/VASP IN HYPERMOTILE RESPONSE OF BREAST CANCER CELL

Several lines of experimental evidence including motility defect of Pfn1,2-null *Dictyostelium* amebae [Haugwitz et al., 1994], Pfn1-mutant *Drosophila* [Verheyen et al., 1994], and Pfn1-deficient human vascular endothelial cells [Ding et al., 2006] all point to a key role of Pfn1 in normal cell migration. Interestingly however, silencing Pfn1 expression leads to increased motility and invasiveness of breast cancer cell lines and conversely, overexpression of Pfn1 dramatically suppresses the aggressive phenotype of breast cancer cells [Roy et al., 2004; Zou et al., 2007]. Taken together, these findings not only suggest that Pfn1's role in cell migration is complex and contextual, but also make Pfn1 an interesting and highly relevant molecule for further investigation in pathological context. Specifically, how reduced Pfn1 expression might contribute to hyper-motile phenotype of breast cancer cells needs to be addressed.

Specific Aim1: ***To determine whether VASP plays a role in the hypermotile response of breast cancer cells induced by loss of Profilin-1 expression.***

This chapter has been published in the following publication:

Bae YH, Ding Z, Zou L, Wells A, Gertler FB and Roy P. (2009). Loss of profilin-1 expression enhances breast cancer cell motility by Ena/VASP proteins. *J Cell Physiol* **219:** 354-364.

4.1 RESULTS

4.1.1 Loss Pfn1 expression leads to faster random motility of MDA-231 breast cancer cells

In our previous study, MDA-231, a highly invasive and metastatic breast cancer cell line, was found to be more motile in both wound-healing and transwell-based migration assays when Pfn1 expression was silenced [Zou et al., 2007]. However, neither of these two migration assays allows for detailed investigation of cell motility and particularly in wound-healing assay, the speed of cell migration can also be influenced by cell-cell contact. Therefore, we examined the effect of Pfn1 knockdown on the motility of MDA-231 cells at the single-cell level to identify possible mechanisms underlying of the resulting increased motility of breast cancer cells. Specifically, we conducted time-lapse imaging of individual MDA-231 cells which were transiently transfected with either a pool of non-targeting control siRNAs or our previously validated siRNA targeting a single region of Pfn1-mRNA [Ding et al., 2006; Zou et al., 2007]. As an additional control, cells were also subjected to mock transfection. Immunoblotting of total cell lysate (TCL) extracted 72 h after siRNA transfection showed strong Pfn1 bands for either of the two control groups of cells, but virtually undetectable signal for Pfn1-siRNA treated MDA-231 cells and HMEC (Fig. 4A). There was also no detectable change in Pfn1 expression between mock and control-siRNA transfection groups. These results demonstrate that we are able to achieve very close to 100% transfection efficiency and near complete suppression of Pfn1 expression in MDA-231 cells and HMEC by siRNA treatment. Figure 4B shows the actual

trajectories of different groups of cells obtained from 2-h time-lapse recordings (data pooled from 3 experiments). From cell trajectory analyses, we found that the average speed of migration of Pfn1-deficient MDA-231 cells (~1.0 μm/min) was 1.9-fold higher than that of mock-transfected (~0.52 μm/min) and control-siRNA treated cells (~0.53 μm/min); there was no significant difference in the average speed of cell migration between our mock and control-siRNA treatment groups thus confirming the specificity of our findings (Fig. 4C). As an additional validation of our results, we repeated these time-lapse motility experiments with a set of pooled siRNAs that targets different regions of Pfn1-mRNA and we found close to 1.5-fold increase in the average speed of MDA-231 cell migration as a result of Pfn1 downregulation (data not shown). A 20% difference in the average speed of migration between single (~1.0 μm/min) and pooled (~0.8 μm/min) Pfn1 siRNA-treated cells could be due to marginally better silencing of Pfn1 achieved with a single siRNA treatment (unpublished observation).

Since breast cancer cells are of epithelial origin, we next analyzed the effect of Pfn1 depletion on the random motility of normal HMEC which express Pfn1 at higher levels than breast cancer cell lines including MDA-231 cells [Janke et al., 2000; Zou et al., 2007] and also show better chemotactic migration in transwell assay in the absence of Pfn1 expression as demonstrated in our previous study [Zou et al., 2007]. Similar to our observation in MDA-231 cells, depletion of Pfn1 in HMEC led to a 2.6-fold increase in the average speed of cell migration in time-lapse assay (Fig. 4C). Overall, these time-lapse motility observations for HMEC and MDA-231 cells are consistent with our previously reported wound-healing and transwell migration data [Zou et al., 2007].

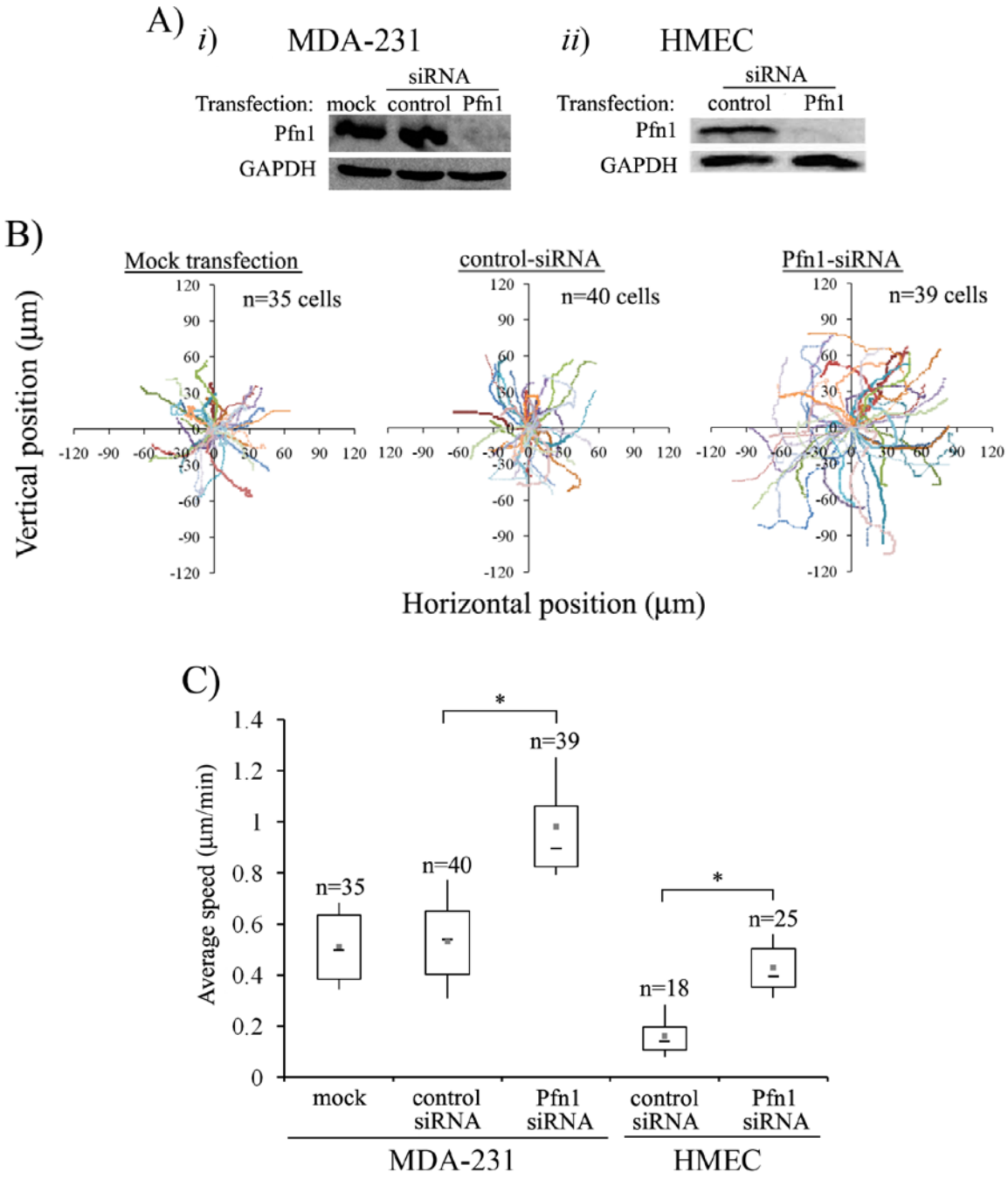

Figure 4: Silencing Pfn1 expression leads to faster motility of MDA-231 breast cancer cells and HMEC in time-lapse assay. A) Pfn1 immunoblot of MDA-231 cell and HMEC lysates 72 h after siRNA transfection (the GAPDH blot serves as the loading control). **B)** Trajectories of individual MDA-231 cells of different experimental groups in time-lapse motility assay (data pooled from three independent experiments). **C)** A box and whisker plot representing the relative comparison of the average speed of migration between different treatment groups for MDA-231 cells and HMEC. All results are normalized to the average value calculated for the control-siRNA treated cells and "n" indicates the number of cells analyzed in each treatment group. The asterisk marks represent $P < 0.05$.

We also asked whether loss of Pfn1 expression affects the directionality of MDA-231 cell movement. From the sequence of images of individual cells for different experimental groups (shown in Fig. 5A), it became apparent that Pfn1-depleted cells change direction of migration less frequently than either of the two control groups of cells. To quantitatively represent this feature, we first scored the change in direction of centroid movement ($\Delta\theta$) as a function of time from which we computed the standard deviation of $\Delta\theta$ (a higher value indicates larger fluctuation in the directionality of movement). As summarized in the form of a box and whisker plot in Figure 5B, a somewhat smaller standard deviation of $\Delta\theta$ of Pfn1-sRNA treated cells compared to either of the two control groups of cells suggests that Pfn1-depletion moderately enhances the directional persistence of motility of MDA-231 cells.

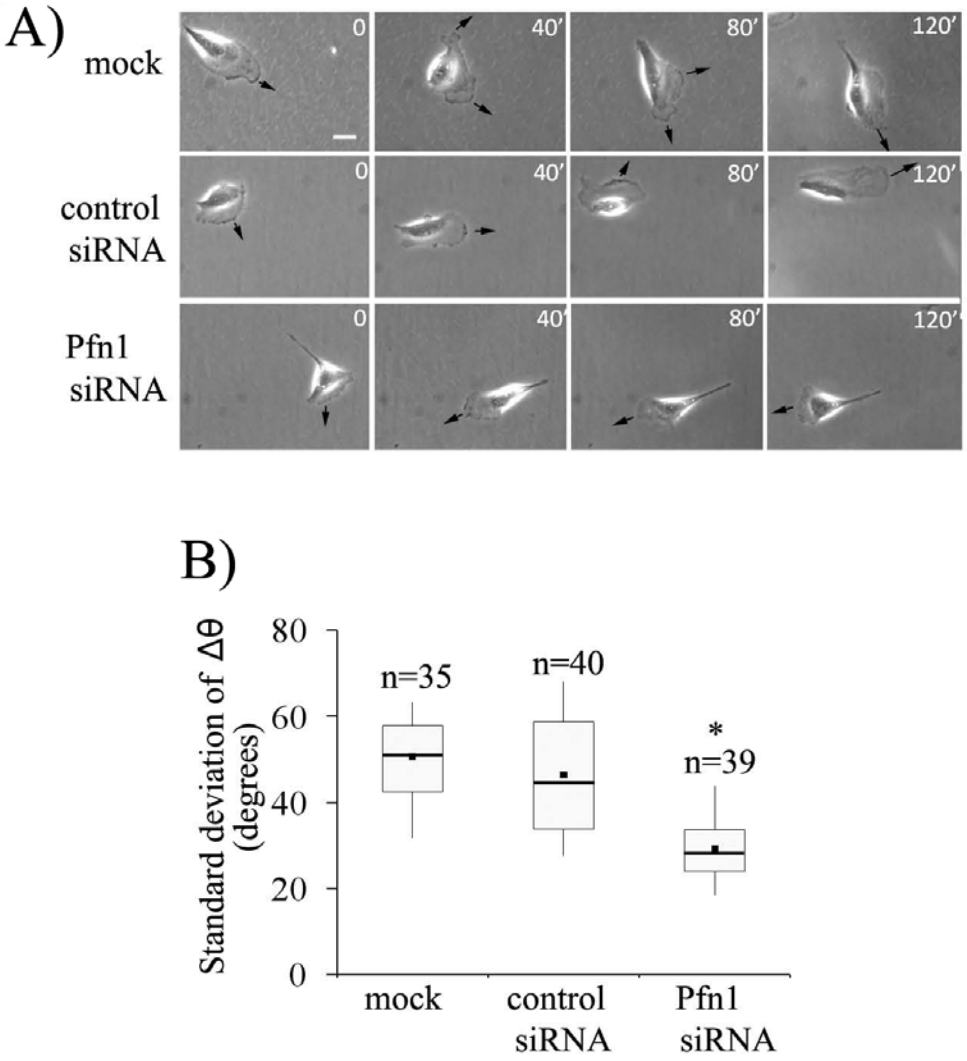

Figure 5: Silencing Pfn1expression enhances directional persistence of MDA-231 cell migration. A) Sequences of images from a set of representative time-lapse experiments of MDA-231 cells conducted for 2 h (arrow- direction of protrusion; scale- 10 μm). **B)** Relative comparison of the standard deviation of Δθ (a measure of the change in the direction of centroid movement) during motility between different treatment groups of MDA-231 cells. The asterisk mark represents $P < 0.05$.

4.1.2 Effect of Pfn1 depletion on lamellipodial protrusion

Lamellipodial protrusion initiates and defines the direction of cell movement. Among its different functions, Pfn1's role has been best described in the context of membrane protrusion during cell migration. We therefore analyzed the leading edge movement of MDA-231 cells for different transfection conditions from kymographs of 1-pixel (0.3 μm) wide lines that were drawn normal to the leading edge and in the direction of protrusion. Figure 6A depicts a set of representative kymographs of the protrusion events of MDA-231 cells for different siRNA transfection conditions where leading edge traces (marked by the arrows) show cycles of typical lamellipodial protrusion and withdrawal (resemble saw-tooth waveforms as outlined by the boxes). Quantitative analyses of kymographs showed that the actual protrusion velocity (this is equal to the slope of the ascending portion of a saw-tooth waveform) of Pfn1-depleted MDA-231 cells (=3.5 μm/min) is almost twofold less than that of control siRNA-treated cells (=7.2 μm/min; Fig. 6B). However, since MDA-231 cells actually exhibit a gain in overall migration speed after Pfn1 depletion, further explanation was needed. During cell motility, a protruding lamellipodium often undergoes partial or complete retraction (also true for MDA-231 cells as shown in Fig. 6A) and therefore it is the net membrane protrusion that correlates with the efficacy of whole cell movement. When we analyzed the rate of net membrane protrusion of MDA-231 cells, we found that Pfn1-deficient cells have a significantly greater net protrusion velocity (=1.0 μm/min) compared to control siRNA treated cells (=0.6 μm/min; Fig. 6C). To explain this observation, we further examined the lamellipodial withdrawal events which showed that on an average, withdrawal of protrusion was more frequent in control (1/min) than in Pfn1-depleted MDA-231 cells (0.5/min; Fig. 6D). Also, the magnitude of lamellipodial withdrawal significantly decreases when Pfn1 expression is suppressed (Fig. 6E).

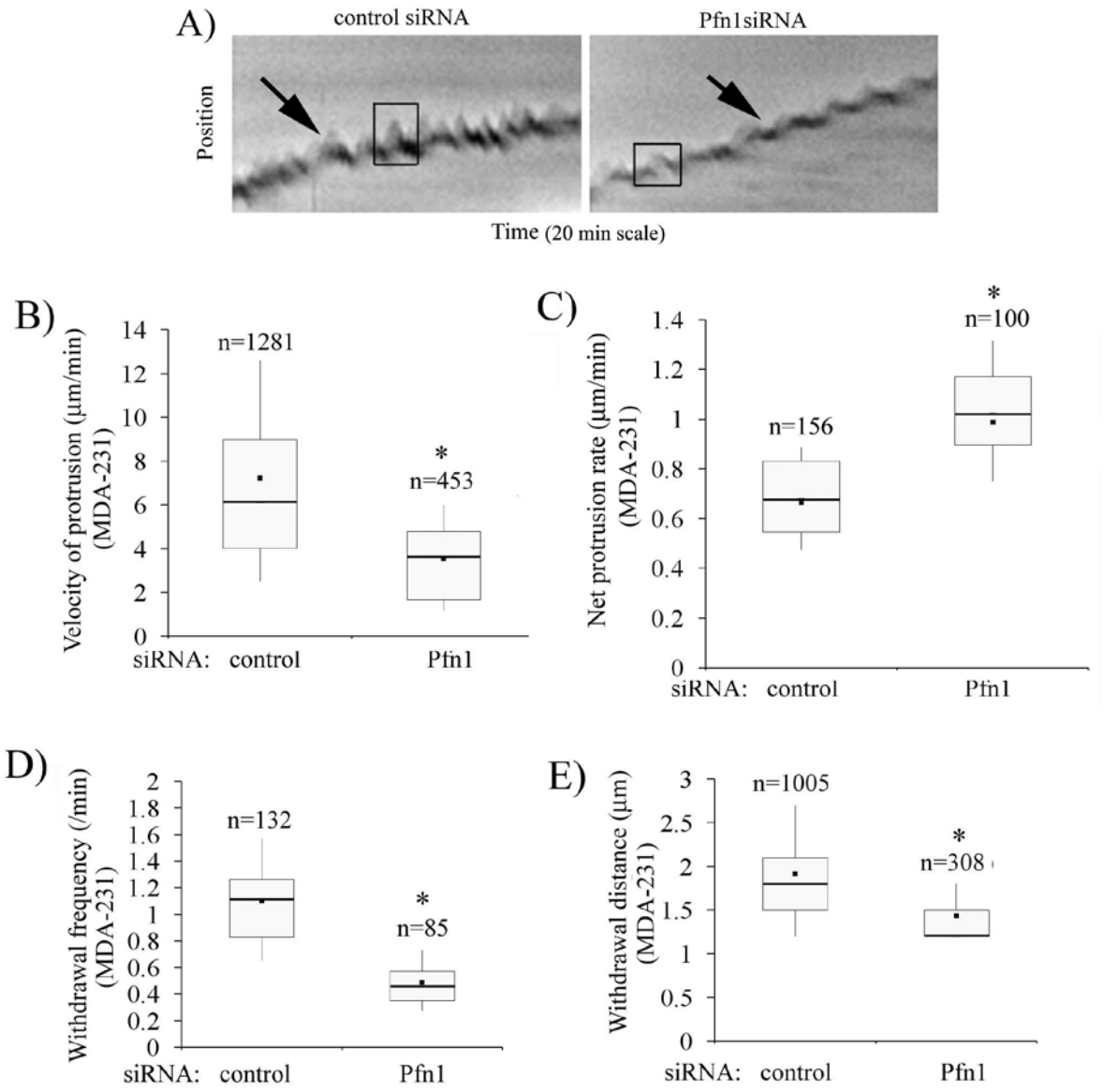

Figure 6: Loss of Pfn1 expression leads to slower but more stable lamellipodial protrusion in MDA-231 cells. A) Kymographs representing lamellipodial dynamics of MDA-231 cells with or without Pfn1 depletion (leading edge traces are marked by the black arrows and the boxes outlining the saw-tooth waveforms represent typical lamellipodial protrusion and withdrawal events). **B)** A box and whisker plots comparing the actual protrusion velocities between control and Pfn1-siRNA treated MDA-231 cells ("n" represents the total number of protrusion events characterized by the saw-tooth waveforms). **C)** A box and whisker plot comparing the net protrusion velocity of MDA-231 cells with or without Pfn1 depletion ("n" indicates the number of kymographs analyzed). **D-E)** Box and whisker plots comparing the frequency (part D) and average distance (part E) of lamellipodial withdrawal (i.e., the descending part of the saw-tooth waveforms) between control and Pfn1-siRNA treated MDA-231cells ("n" in parts D and E represent the total number of kymographs and withdrawal events, respectively). These data are based on analyses of 30 cells for each transfection condition pooled from three independent experiments. The asterisk marks represent $P < 0.05$.

4.1.3 Silencing Pfn1 expression enhances VASP localization at the leading edge

Stable lamellipodial protrusion is one of the characteristic features of smooth and gliding type of cell movement. It has been recently shown that fish keratocytes (an extremely fast migrating epithelial cell type) migrate faster and in a smooth, gliding fashion when Ena/VASP family proteins are enriched at their leading edge [Lacayo et al., 2007]. Leading edge targeting of Ena/VASP has also been shown to result in faster membrane protrusion [Bear et al., 2002]. We therefore asked whether sub-cellular distribution of Ena/VASP in MDA-231 cells is altered by Pfn1-depletion. We focused on VASP because it is the most well-characterized member of the protein family. Since VASP is recruited to the leading edge in a protrusion-dependent manner, we performed costaining of VASP and phalloidin (to identify the leading edge of lamellipodia) of MDA-231 cells under different siRNA transfection conditions. Only those cells which formed prominent lamellipodia (identified from phalloidin-stained images) were selected for comparison of VASP distribution between the different treatment groups (Fig. 7A). VASP was localized at the leading edge of lamellipodia (arrowheads), focal adhesions (thick arrows) and occasionally, in dorsal ruffles (thin arrow). VASP signal at the very leading edge of lamellipodia was found to be conspicuously higher in Pfn1-depleted cells. Fluorescence intensity analyses of line scans across the leading edge showed that the average signal intensity of VASP at the very leading edge is almost fourfold higher in Pfn1-depleted cells than in control-siRNA treated cells (Fig. 7B). Immunoblot analyses confirmed that silencing Pfn1 expression does not alter the overall expression level of VASP in MDA-231 cells (Fig. 7C). Since VASP binds to barbed ends of actin filaments [Bear et al., 2002] and previous studies have shown that cofilin, an F-actin severing protein, plays a key role in generating barbed ends of actin filaments in breast cancer cells [Chan et al., 2000], we also compared the expression level of cofilin between control and

Pfn1-depleted cells. Immunoblot data showed that cofilin expression in MDA-231 cells is not altered by Pfn1 depletion [Fig. 7C]. It is, however, noteworthy here that Pfn1 depletion results in a slight reduction in the total actin level in MDA-231 cells as demonstrated previously by our group [Zou et al., 2007]. Finally, to determine whether stronger VASP localization at the leading edge as a result of Pfn1 depletion is a reproducible feature in other cell types, we performed similar immunostaining experiments with HUVEC and normal HMEC. Interestingly, both cell lines also showed stronger VASP signal at the leading edge in the absence of Pfn1 expression therefore substantiating our findings (Fig. 7D).

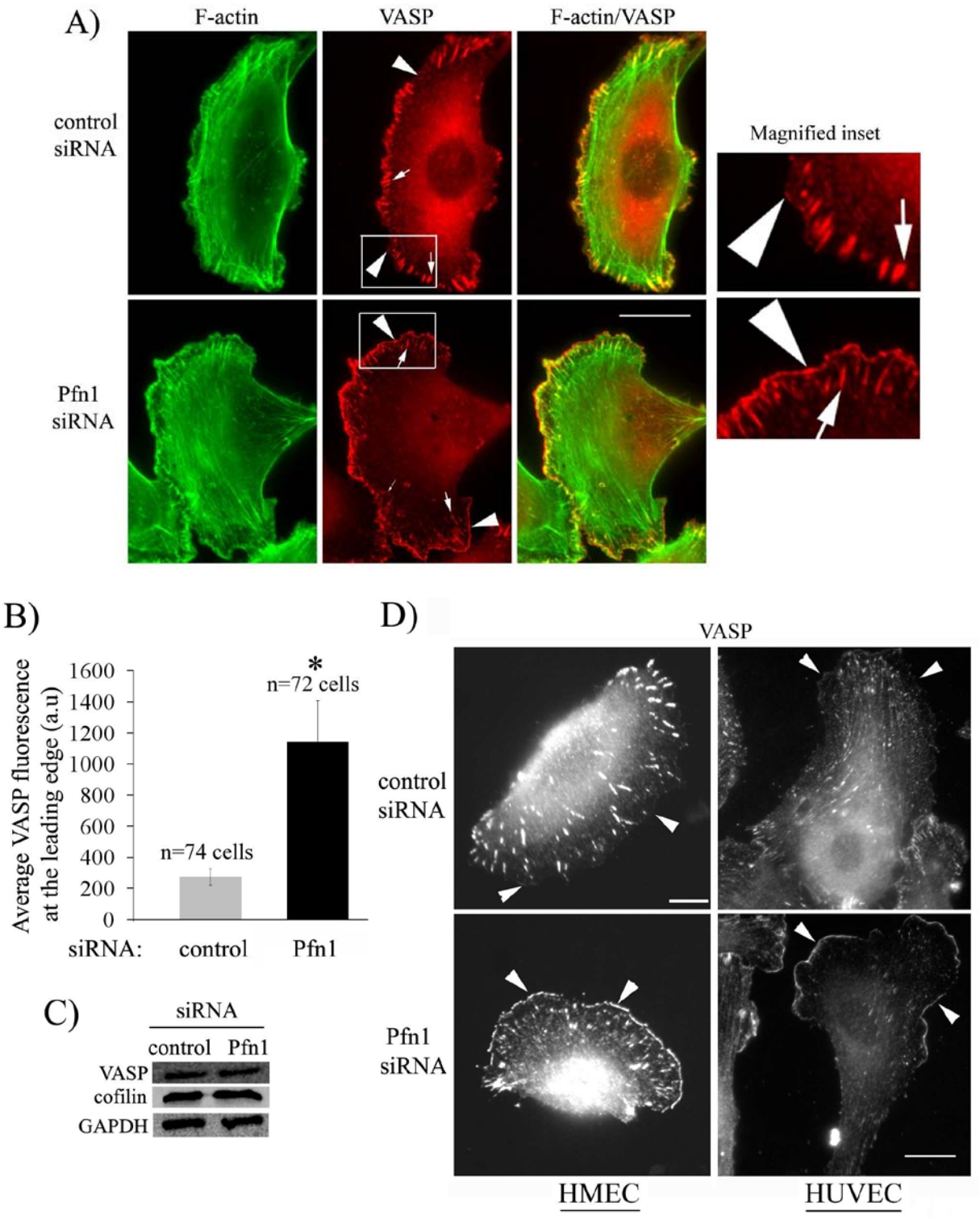

Figure 7: Silencing Pfn1 expression enhances leading edge localization of VASP. A) VASP (red) and phalloidin (green) costaining of MDA-231 cells show stronger leading edge (arrowhead) localization of VASP in Pfn1-deficient cells (VASP localization at focal adhesion and ruffles are marked by thick and thin arrows, respectively; scale- 10 µm). Magnified forms of

the insets (outlined by the boxes) are displayed in the right most parts. **B)** A bar graph comparing the relative intensity of VASP staining at the lamellipodial edge between control and Pfn1-depleted MDA-231 cells (a.u., arbitrary units; data summarized from two independent experiments and the asterisk mark denotes $P < 0.05$). **C)** Silencing Pfn1 does not alter the total expression level of VASP and cofilin in MDA-231 cells (GAPDH blot serves as the loading control). **D)** VASP immunostaining of HMEC and HUVEC show similar VASP enhancement at the leading edge as a result of Pfn1 depletion. Scale bars in all images represent 20 μm.

4.1.4 Ena/VASP is responsible for hypermotile phenotype of Pfn1-deficient MDA-231 cells

Inhibition of Ena/VASP function leads to cell-type specific changes in cell migration. Leading edge targeting of VASP correlates with faster migration of fish keratocytes [Lacayo et al., 2007], but in the case of fibroblasts, inhibition or deletion of Ena/VASP results in increased motility [Bear et al., 2000]. To determine whether lamellipodial targeting of VASP is responsible for creating hyper-motile phenotype of Pfn1-deficient MDA231 cells, we adopted a previously described strategy to inhibit Ena/VASP function by expressing Ena-VASP homology-1 (EVH1) binding motifs of ActA fused to a mitochondrial membrane anchor (EGFP-FPPPP-mito: referred to as "FP4-mito"). This particular construct effectively depletes all Ena/VASP proteins from their normal sites of function and sequesters them on mitochondria [Bear et al., 2000]. A similarly structured construct deficient in binding to Ena/VASP proteins (EGFP-APPPP-mito: referred to as "AP4-mito") was used as a control. To demonstrate the efficacy of this construct in our cell system, we transfected Pfn1-siRNA treated MDA-231 cells with either AP4-mito or FP4-mito construct and then examined VASP localization by immunostaining (Fig. 8). As expected, VASP distribution was not affected by expression of the AP4-mito construct: Pfn1-siRNA transfected cells bearing this construct still displayed strong VASP staining at their leading edges. However, cells expressing FP4-mito showed no VASP signal at the leading edge or in focal adhesions and instead exhibited the expected mitochondrial sequestration of VASP (specificity and efficacy of these two constructs were also confirmed for control-siRNA treated cells in a similar manner- data not shown).

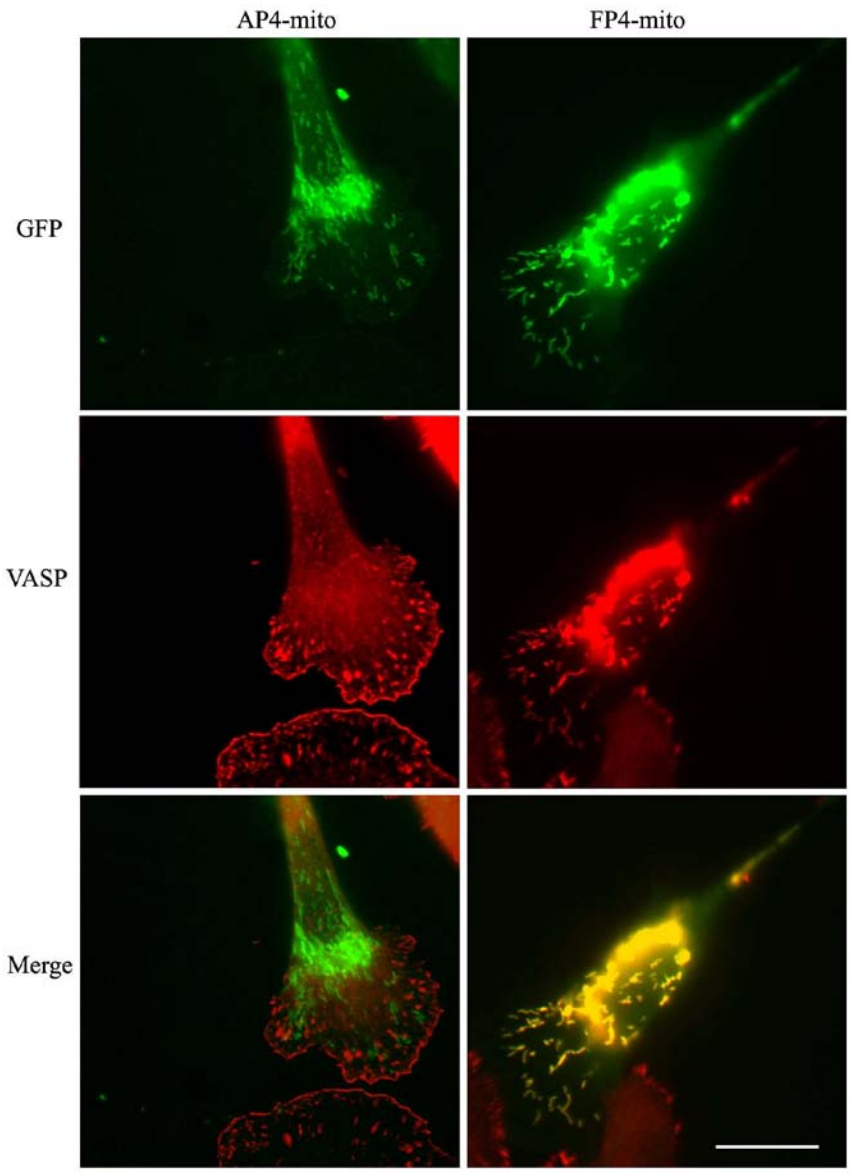

Figure 8: Effects of expression of EGFP-FP4/AP4-mito on VASP localization in Pfn1-deficient MDA-231 cells. GFP (green) images of Pfn1-siRNA treated cells show typical mitochondrial localization of AP4-mito and FP4-mito fusion proteins. Corresponding VASP immunostaining (red) images show that VASP's localization to the leading edge and focal adhesion are affected only by FP4-mito expression. Merged images reveal complete colocalization of VASP with FP4-mito (appears yellow) but not with AP4-mito (scale- 20 μm).

Next, we performed time-lapse imaging of control and Pfn1-siRNA bearing MDA-231 cells following transfection with either AP4-mito or FP4-mito construct and compared the migration speed of EGFP-negative (only carries siRNA) and EGFP-positive (expresses either AP4-mito or FP4-mito against siRNA background) cells. Figure 9A shows that for either of the siRNA treatment groups, there was no significant difference in the average speed of migration between EGFP-negative and the corresponding AP4-mito bearing cells. Expression of FP4-mito reduced the average speed of migration of control siRNA treated cells by a nominal 15% although this difference was not statistically significant. The average speed of AP4-mito expressing Pfn1-depleted cells was 50% higher compared to the corresponding control siRNA-treated cells. The FP4-mito construct, however, reduced the speed of Pfn1-deficient cells by nearly 65%; the average speed of these cells was in fact 40% less than that of FP4-mito bearing control siRNA treated cells. Overall these data suggest that Ena/VASP compensates for the loss of Pfn1 and further augments the overall motility of MDA-231 cells when Pfn1 expression is silenced.

Since Ena/VASP sequestration in Pfn1-deficient cells leads to a dramatic inhibition in motility, we speculated that lamellipodial protrusion of these cells might be compromised. To confirm this, we studied the leading edge dynamics of Pfn1-depleted MDA-231 cells with or without Ena/VASP sequestration. We found that the kymograph patterns of EGFP-negative and AP4-mito expressing cells were very similar; however FP4-mito expressing cells exhibited significant reduction in protrusion (as judged from a near-flat profile- Fig. 9B). Data analyses showed that Ena/VASP inhibition by FP4-mito resulted in nearly 70% reduction in the net protrusion velocity of Pfn1-defiicient MDA-231 cells (Fig. 9C), suggesting that lamellipodial targeting of Ena/VASP plays a major role in the protrusive activity of these cells.

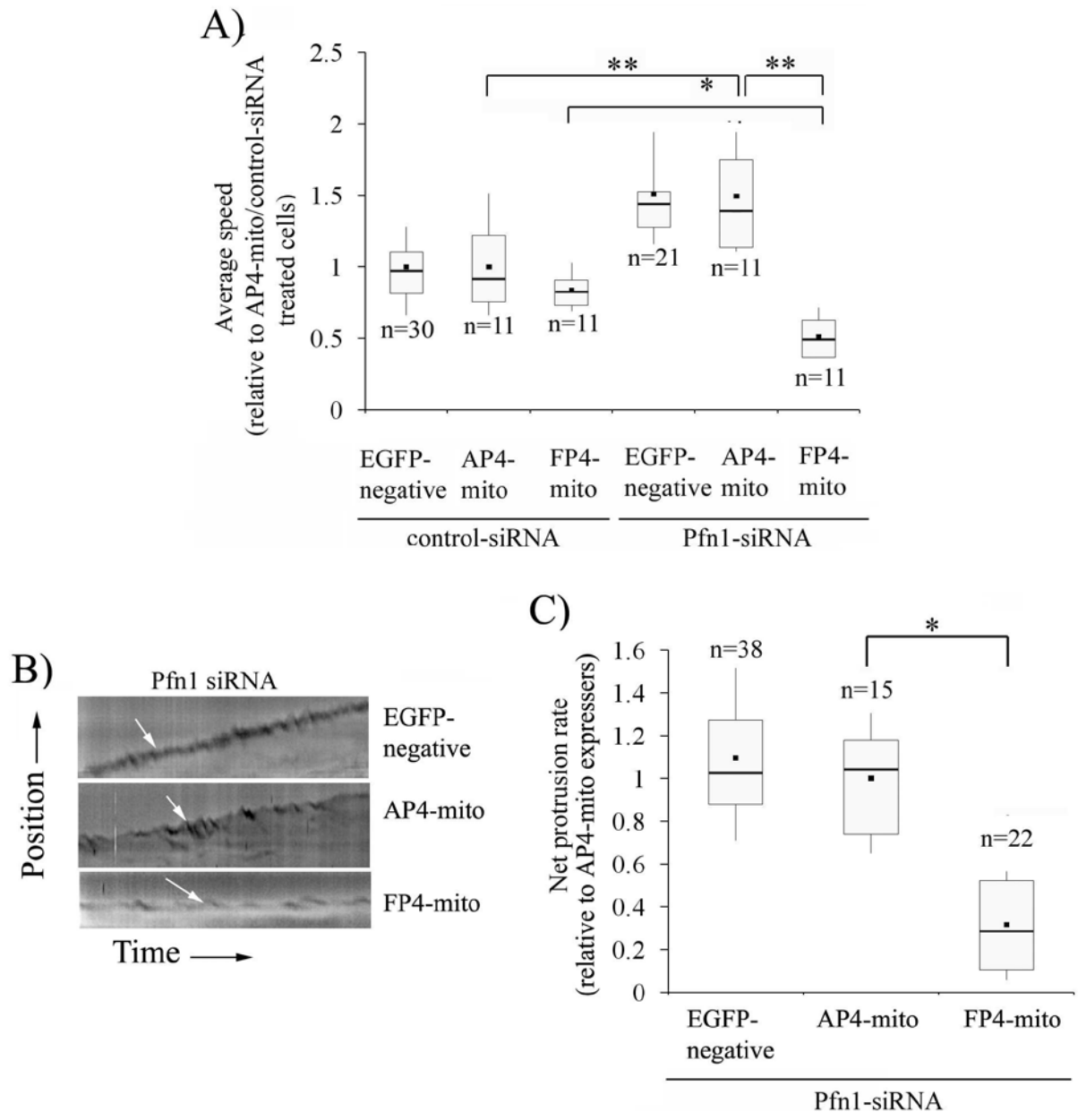

Figure 9: Mitochondrial sequestration of Ena/VASP dramatically impairs the motility and lamellipodial protrusion of Pfn1-deficient MDA-231cells. A) A box-whisker plot summarizes the relative speed of control and Pfn1-siRNA treated cells with (FP4-mito) or without (either AP4-mito or EGFP-negative) mitochondrial sequestration of Ena/VASP (all data are normalized to AP-mito expressing control siRNA treated cells; "n" represents the number of cells analyzed for each group pooled from three independent 2-h long time-lapse experiments). The single and double asterisks represent $P < 0.05$ and $P < 0.01$, respectively. **B)** Representative kymographs showing leading edge traces (white arrows) of Pfn1-depleted MDA-231 cells with or without Ena/VASP inhibition. **C)** A box and whisker plot comparing the net protrusion velocities between the different treatment groups of Pfn1-deficient cells (data normalized to AP4-mito expressing cells and "n" indicates the number of cells in each group pooled from three-independent experiments; $*P < 0.05$).

Ena/VASP proteins bind to the barbed ends of actin filaments and support actin polymerization in the presence of actin filament capping proteins [Barzik et al., 2005; Pasic et al., 2008]. This has been proposed to be the mechanism underlying Ena/VASP-driven membrane protrusion. Leading edge localization of VASP in fibroblasts and keratocytes requires free barbed ends of growing actin filaments [Bear et al., 2002; Lacayo et al., 2007]. In our case, when we treated Pfn1-depleted MDA-231 cells with 100 nM cytochalasin D (CD; under these conditions CD works mainly as a pharmacological barbed-end capper without causing significant depolymerization of actin filaments [Bear et al., 2002]) for 30 min, VASP became completely delocalized from the leading edge while treatment with carrier DMSO had not effect at all (Fig. 10). Phalloidin counterstaining confirmed that 100 nM CD treatment did not cause any major depolymerization of actin filaments; also the characteristic fan-shaped lamellipodial structure (arrow) was seen to be preserved. Antagonistic action of CD on lamellipodial targeting of VASP is consistent with VASP's binding to the barbed ends of actin filaments as expected.

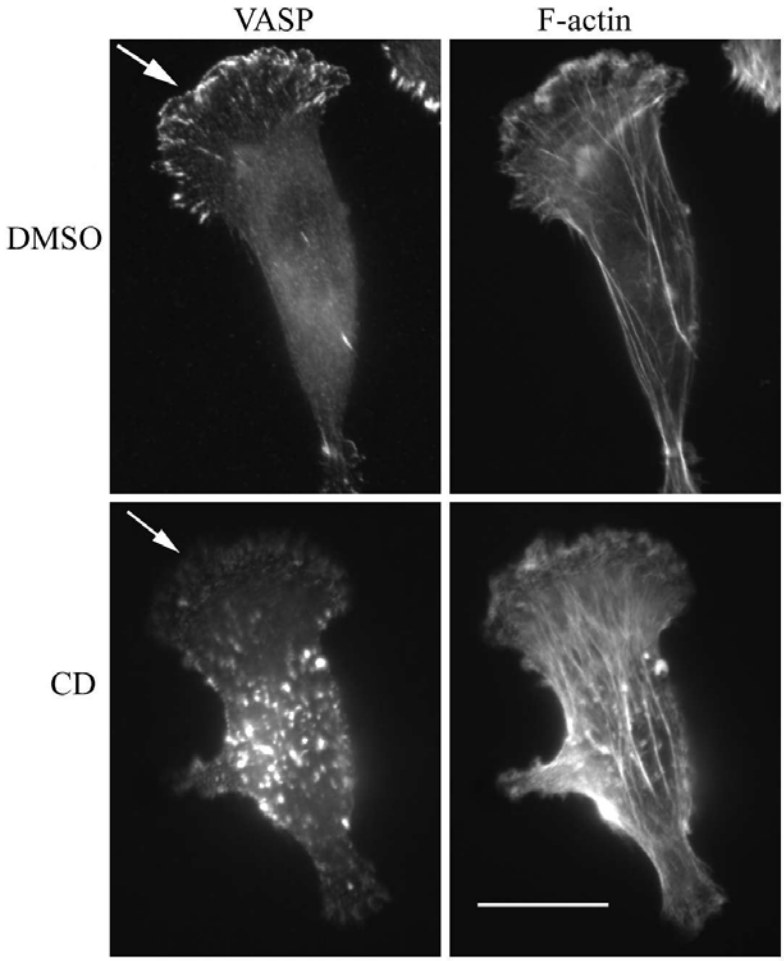

Figure 10: Lamellipodial targeting of VASP in Pfn1-deficient MDA-231 cells is sensitive to low dose of cytochalasin-D (CD) treatment. VASP immunostaining images of Pfn1-deficient cells show that VASP is completely delocalized from the leading edge (arrow) when exposed to 100 nM CD for 30 minutes while diluent DMSO treatment has no effect. F-actin counterstaining by phalloidin show that 100 nM CD does not lead to any major depolymerization of actin filaments or disruption of lamellipodia (scale - 20 μm).

4.2 DISCUSSION

Gain-of-motility of certain types of adenocarcinoma cells induced by loss of Pfn1 expression has been previously reported by us and others [Wu et al., 2006; Zou et al., 2007]; but, the mechanisms underlying this effect have not been delineated yet. This has been challenging particularly since Pfn1 has been traditionally viewed as a molecule required for cell migration. This study was the first attempt to identify a possible mechanism of how reduced Pfn1 expression could actually promote migration of breast cancer cells.

Our time-lapse data revealed that silencing Pfn1 expression leads to faster motility of both MDA-231 breast cancer cells and normal HMEC. This is in contrast to the behavior of HUVEC which exhibit significantly reduced motility after Pfn1 depletion as shown by our group in a previous study [Ding et al., 2006]. To better understand the physical basis for cell-specific difference in the overall motility response resulting from Pfn1 depletion, we studied the lamellipodial dynamics of HUVEC [Bae et al., 2009] and MDA-231 cells and found that in both cell types, the actual protrusion velocity is reduced when Pfn1 expression is suppressed. This is the first direct demonstration of the effect of Pfn1 depletion on the actual protrusion velocity of cells, and is consistent with previously shown slower intracellular propulsion of bacterial pathogens in the absence of Pfn1 [Loisel et al., 1999; Mimuro et al., 2000]. Interestingly, Pfn1-deficient MDA-231 cells showed less withdrawal of protrusion, both in terms of its frequency and magnitude, compared to control cells which eventually resulted in a more effective net protrusion and an overall increase in motility.

We found a striking enrichment of VASP at the very leading edge of MDA-231 cells as a consequence of Pfn1 depletion, and this finding was also reproducible in both HMEC and HUVEC. We further showed that specifically Pfn1-deficient but not control MDA-231 cells

become severely impaired in motility when Ena/VASP function is inhibited by mitochondrial sequestration. These data imply that (1) Pfn1 by itself still acts as a pro-migratory molecule in MDA-231 cells as literature has demonstrated in other cell types (Haugwitz et al., 1994; Ding et al., 2006), and (2) it is the enhanced Ena/VASP localization at the leading edge which rescues and further augments the overall motility of MDA-231 cells when Pfn1 expression is silenced. Although we have only studied VASP localization in this study, the other two Ena/VASP proteins, Mena and EVL have overlapping functions and localization with VASP. Therefore, it is likely that Mena also contributes to the hypermotile phenotype of Pfn1-deficient cells as it is expressed robustly in MDA-231 cells (unpublished observation in Dr. Gertler laboratory). The mitochondrial sequestering construct used in this study is effective against all three members of Ena/VASP protein family; whether there are any differences in the contributions of Mena or VASP to the phenotype of Pfn1-deficient cells remains to be determined.

Ena/VASP proteins have a well-established role in promoting membrane protrusion [Rottner et al., 1999]. Previous studies showed that Ena/VASP increases the speed of intracellular actin-driven propulsion of Listeria monocytogenes [Laurent et al., 1999; Geese et al., 2002] and leading edge targeting of VASP correlates with faster protrusion in cells [Bear et al., 2002; Lacayo et al., 2007]. Mitochondrial sequestration of Ena/VASP leading to reduced membrane protrusion in Pfn1-deficient MDA-231 cells is consistent with those findings. Ena/VASP can bind Pfn1-actin complexes in an orientation favorable for transfer of monomer to growing barbed ends. Ena/VASP is known to facilitate actin polymerization by antagonizing the action of F-actin capping proteins [Bear et al., 2002]; the anti-capping activity does not require Pfn, but is enhanced by the presence of Pfn [Barzik et al., 2005]. In the present case, leading edge targeting of VASP facilitates lamellipodial protrusion in a near absence of Pfn1 expression.

In a previous study, we failed to detect Pfn2 expression in MDA-231 cells at least by immunoblotting [Zou et al., 2007]. Although it is possible that very low levels of residual Pfn1 or Pfn2 enhance VASP-dependent actin polymerization, the contribution should be minimal. Therefore, it is likely that VASP drives membrane protrusion via Pfn-independent anti-capping action.

The effect of Ena/VASP perturbation on the overall cell motility is cell-type dependent. This apparent discrepancy between different model systems is not completely surprising. Although the actual protrusion velocity increases when VASP is targeted to the leading edge, the overall persistence of protrusion and the net cell movement decrease in the case of slow-moving fibroblasts. This is because VASP-mediated protrusions in fibroblasts tend to be unstable and are prone to withdrawal [Bear et al., 2002]. The lamellipodial dynamics of rapidly migrating cell types such as fish epithelial keratocytes show much less oscillatory behavior when compared to fibroblasts, and therefore, the overall motility response of these cells to leading edge targeting of VASP can be quite different. Interestingly, our data showed that protrusions generated by Pfn1-deficient MDA-231 cells are less susceptible to withdrawal therefore implying enhanced stability of these protrusions, and this is likely to be a result of better protrusion-adhesion coupling. Although the underlying mechanism is not clear, one simple explanation could be that since Pfn1-silenced cells protrude slower, these protrusions may have a better chance of engagement to the underlying substrate via adhesion receptors.

A key question remaining to be investigated in detail is how absence of Pfn1 expression leads to VASP enrichment at the leading edge. One possibility is that both control and Pfn1-depleted cells have comparable efficiency of targeting VASP to the membrane during protrusion. Since Pfn1-depleted cells show evidence of less withdrawal of protrusion, it is possible that

VASP-rich protruding membrane is better sustained and represented in fixed-cell preparations, as in immunostaining experiments. However, a comparable efficiency of targeting VASP to the leading edge is unlikely to result in a fourfold difference in membrane staining of VASP between control and Pfn1-depleted MDA-231 cells. An alternative explanation that we favor is that silencing Pfn1 expression actually increases the membrane targeting efficiency of VASP. Since a deletion mutant of VASP lacking its polyproline domain (a region that binds to Pfn1) targets normally to the leading edge [Loureiro et al., 2002], Pfn1 is unlikely to have a direct effect on Ena/VASP targeting to the leading edge. Therefore, we think loss of Pfn1 expression enhances leading edge targeting of VASP through an indirect mechanism, possibly involving Lpd as to be examined in specific Aim 2.

In conclusion, we have now identified a possible mechanism of how loss of expression of a pro-migratory molecule like Pfn1 can result in increased migration of breast cancer cells through enhanced lamellipodial targeting of Ena/VASP proteins. We will need to determine the generalizability of our findings by expanding our studies to other breast cancer cell lines and other types of adenocarcinoma that have reduced Pfn1 expression compared to their normal counterparts.

5.0 PHOSPHOINOSITIDE-INTERACTION MEDIATED INHIBITORY ACTION OF PROFILIN-1 ON BREAST CANCER CELL MIGRATION

A key cellular function downstream of membrane D3-PPI signaling events is the regulation of actin cytoskeletal dynamics which is critical for overall cell motility [Blume-Jensen et al., 2001]. During tumor progression, this cellular function of D3-PPI becomes dysregulated. Among the D3-PPI groups, PIP_3 has been mostly studied in *Dictyostelium* and *neutrophil* model systems in the context of directional sensing and motility during chemotaxis. However, a major gap in the literature is the lack of understanding of specific signaling functions of membrane $PI(3,4)P_2$ (another byproduct of PI3K signaling) in cancer cell motility. Recently, lamellipodin (Lpd; an adaptor protein which binds to and recruits Ena/VASP family protein to the leading edge), has been identified and noted that it binds to pH domain of $PI(3,4)P_2$ with high selectivity [Krause et al., 2004]. Ena/VASP localization at the leading edge associates with faster and in a smooth, gliding fashion of migration in fish keratocytes [Lacayo et al., 2007]. One of the possible links between D3-PPI signaling and regulation of actin dynamics at the leading edge of migrating cells is Lpd-mediated VASP recruitment and this needs to be investigated.

Specific Aim2: ***To examine whether Pfn1 inhibits breast cancer cell motility by regulating D3-phosphoinositide availability for lamellipodin targeting to the membrane.***

Some of the contents in this chapter have been or will be published in the following publications:

Bae YH, Ding Z, Zou L, Wells A, Gertler F, Roy P. (2009). Loss of profilin-1 expression enhances breast cancer cell motility by Ena/VASP proteins. *J Cell Physiol* **219:** 354-364.

Bae YH, Ding Z, Das T, Wells A, Gertler FB, Roy P. Membrane PI(3,4)P_2 availability, regulated by profilin-1, impacts breast cancer cell motility secondary to lamellipodin binding. [Under Review: 02/2010]

5.1 RESULTS

5.1.1 Pfn1 inhibits breast cancer cell motility by negatively regulating VASP/Lpd targeting to the leading edge

Lpd, a protein that contains a PH (pleckstrin-homology) domain with affinity for PI(3,4)P_2, has been identified as one of the potential linkers for targeting Ena/VASP close to the plasma membrane at the leading edge and at least for fibroblasts, Lpd has been shown to play an important role in membrane protrusion [Krause et al., 2004]. Lpd staining of Pfn1-siRNA treated MDA-231 cells showed its localization at the lamellipodial tip (arrows) and ruffles (arrowheads-Fig. 11A). There was also a very strong colocalization of Lpd and VASP at the leading edge (Fig. 11A). As shown previously in fibroblasts [Krause et al., 2004], Lpd targeting to the leading edge in our cells is not VASP-dependent since expressing FP4-mito that sequesters Ena/VASP to mitochondria still preserves strong leading edge staining of Lpd (Fig. 11B). To determine whether Lpd plays a role in VASP targeting to the leading edge in Pfn1-depleted MDA-231 cells we transfected MDA-231 cells with Pfn1-siRNA either alone or together with Lpd-siRNA. We found that co-suppression of Lpd and Pfn1 expression in MDA-231 cells by dual siRNA treatment (Fig. 11C) results in markedly reduced VASP distribution at the leading edge (Fig. 11D) thus confirming critical requirement of Lpd for lamellipodial targeting of VASP in our cell line.

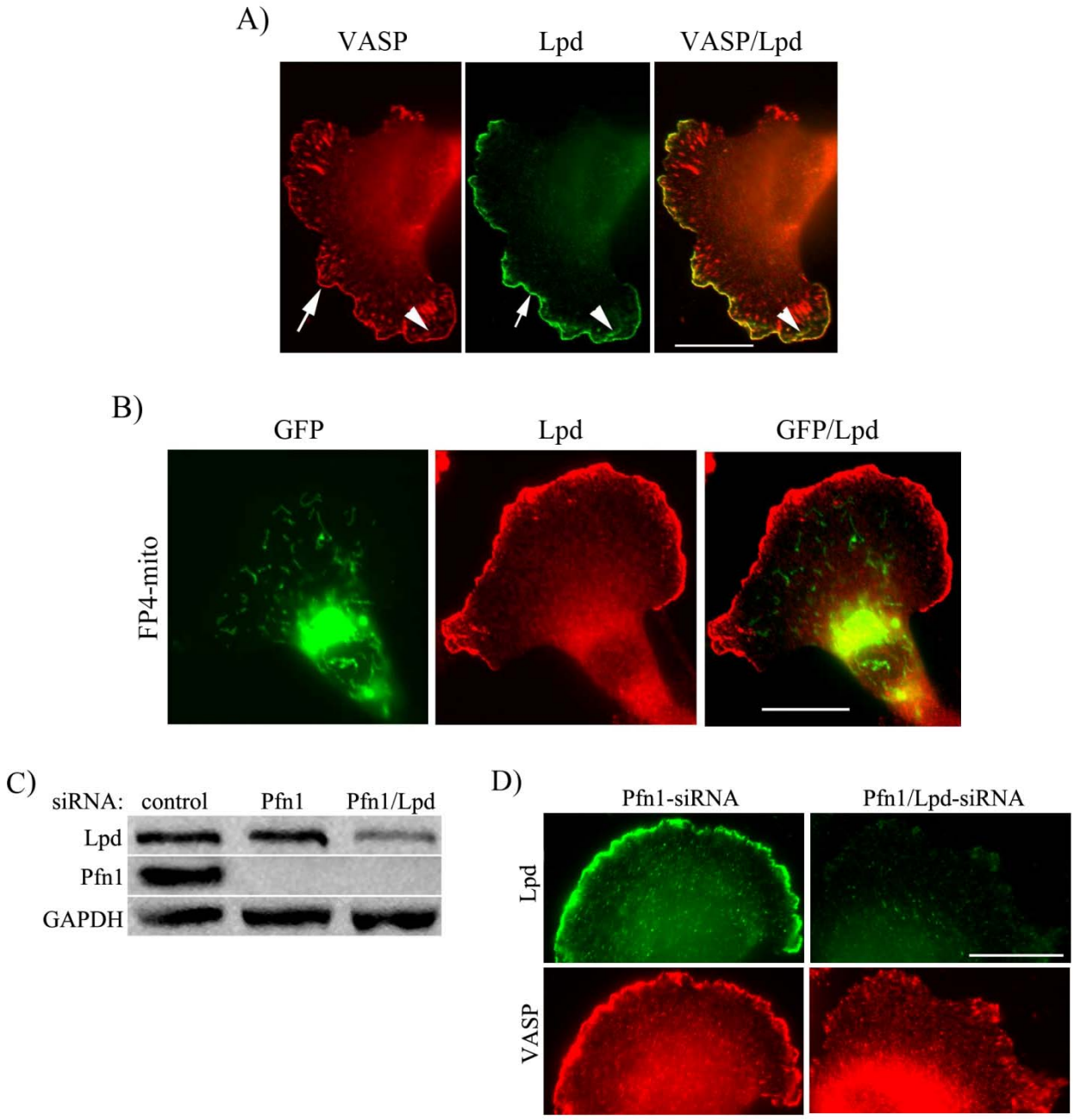

Figure 11: VASP is colocalized with Lpd at the leading edge in Pfn1-deficient cells. A) Immunostaining shows complete colocalization of VASP (red) and Lpd(green) at the leading edge (arrows) in Pfn1 depleted MDA-231 cells (appears yellow in the merged image). **B)** Pfn1-silenced MDA-231 cells expressing FP4-mito (green) maintain strong leading edge targeting of Lpd (red). The merged image in the right most part shows no overlapping of these two fluorescence signals. **C)** Immunoblot data showing dual suppression of Lpd and Pfn1 in MDA-231 cells by siRNA cotransfection (GAPDH blot - loading control). **D)** VASP and Lpd costaining of MDA-231 cells transfected with Pfn1 siRNA either alone or together with Lpd siRNA.

Next, we observed that silencing Pfn1 leads to a significant 4-fold increase in Lpd distribution at the leading edge in MDA-231 cells, and conversely, MDA-231 cells stably overexpressing GFP-Pfn1 about two-fold [Smith et al., 2010] present 25% less Lpd content at the lamellipodial tip when compared to the corresponding control GFP expressers (Fig. 12A and Fig. 12B). Note that loss of Pfn1 expression has no effect on the overall expression of Lpd in MDA-231 cells (Fig. 12C). We additionally found that Lpd enrichment at the leading edge induced by silencing of Pfn1 is reproducible in at least two other cell types including normal HMEC and HUVEC (human umbilical vein endothelial) (Fig. 12D). Interestingly, while the HMEC are similarly hypermotile upon Pfn1 depletion, [Bae et al, 2009], the HUVEC become hypomotile [Ding et al., 2006]. Thus, Pfn1-dependent regulation of Lpd localization appears be a generalized phenomenon.

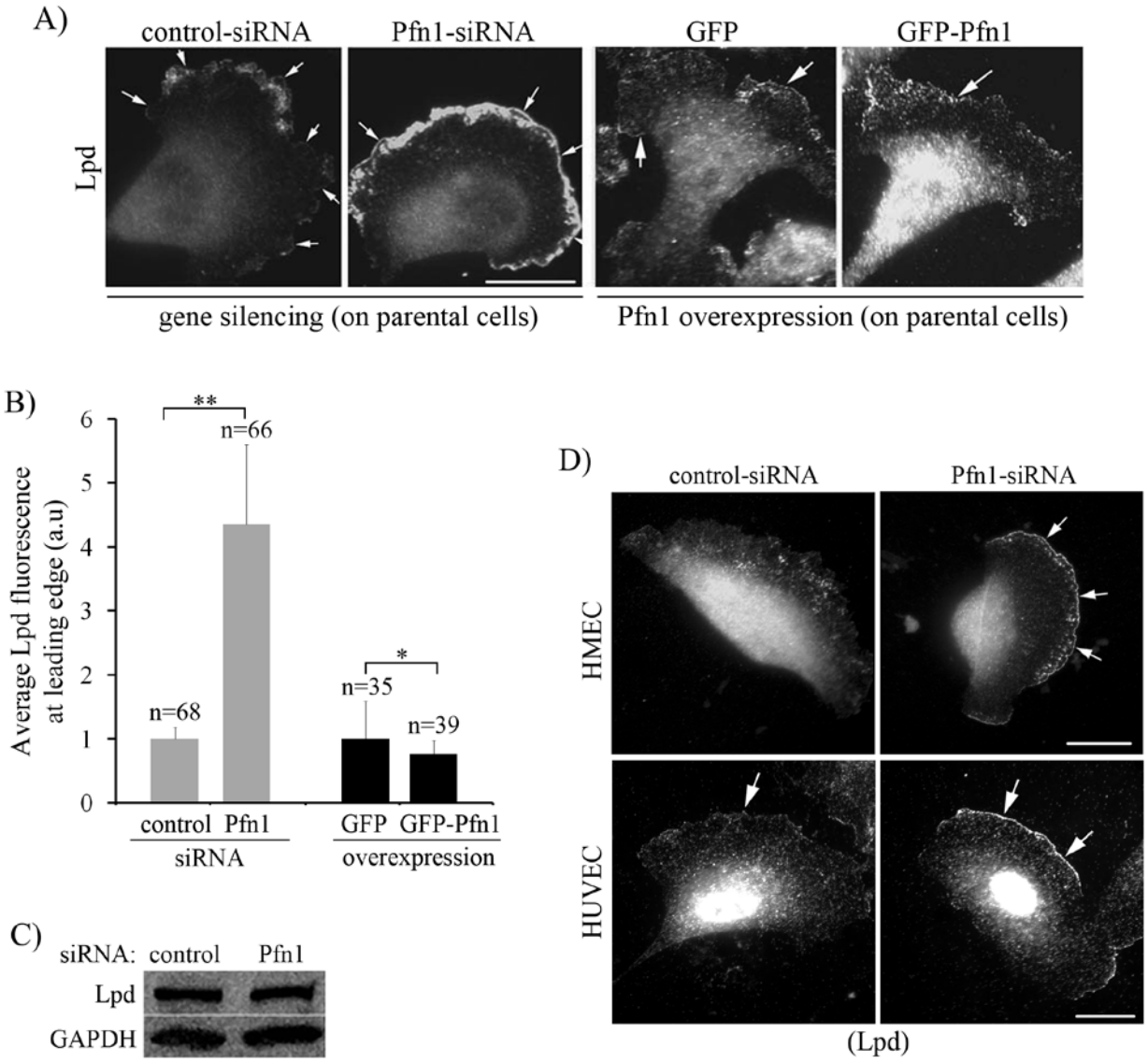

Figure 12: Pfn1 is a negative regulator of lamellipodial targeting of Lpd. A) Lpd immunostaining data showing the effects of silencing and stable overexpression of Pfn1 in parental MDA-231 cells on Lpd localization at the leading edge (arrows). **B)** A bar graph comparing the relative intensity of Lpd staining at the lamellipodial edge in MDA-231 cells after silencing (grey bars) and overexpression (black bars) of Pfn1 ('n' - number of cells analyzed; **: $p<0.01$; *: $p<0.05$). **C)** Immunoblot showing comparable Lpd level between control and Pfn1-siRNA treated MDA-231 cells (GAPDH blot - loading control). **D)** Lpd immunostaining showing Lpd enrichment at the lamellipodial tip in response to Pfn1-siRNA treatment in both normal HMEC and HUVEC (arrow) (scale bar - 20μm).

We next asked whether Lpd plays a role in the hypermotile response of Pfn1-depleted MDA-231 cells. Previously, Lpd knockdown was shown to cause impaired lamellipodia formation and reduce velocity of protrusion in fibroblasts [Krause et al, 2004]. When we compared morphology of control and Lpd-siRNA treated MDA-231 cells on tissue-culture substrate without any ECM coating, we also found that limiting Lpd expression somewhat decreases the overall flare of lamellipodial protrusion (as judged by the narrowing of lamellipod in Lpd knockdown cells) (Fig. 13A). Phenotypic change induced by Lpd suppression appears to be more prominent when Pfn1 expression is simultaneously downregulated as many cells in this group even fail to form proper lamellipodia (Fig. 13A). Interestingly, when the same groups of cells are seeded on collagen-coated substrate (mimics the substrate condition for motility experiments), Lpd knockdown alone does not appear to have any significant morphological consequence in MDA-231 cells as judged by normal appearing lamellipodia in both control and Lpd-siRNA treated cells, and only a small difference (~8%) in the fraction of cells with lamellipodia formation between the two groups (Fig. 13B). In the same experimental setting, lamellipodia formation in Pfn1-deficient cells, however, appears to be still significantly inhibited by Lpd knockdown as judged by a significant 31% lower fraction of cells forming lamellipodia (Fig. 13B). Consistent with these phenotypic distinctions, time-lapse migration assay showed that limiting Lpd expression does not have any significant effect on the motility of parental MDA-231 cells, but drastically reduces the average speed of Pfn1-deficient cells (Fig. 13C). These data demonstrate that hypermotile response of MDA-231 cells induced by Pfn1-downregulation is Lpd-mediated. Differential sensitivity between control vs Pfn1 knockdown cells to Lpd depletion could be due to possible compensatory action by other Pfn1-binding Lpd-homolog proteins as elaborated in the discussion. Given that lamellipodia formation/protrusion is

driven largely by actin polymerization, we next examined the effect of Lpd depletion on actin cytsokeletal structure in Pfn1-defiicient cells by phalloidin staining. We found that Lpd knockdown results in significantly reduced F-actin content at the leading edge (as judged by the intensity of phalloidin staining – Fig. 13D) and a concomitant ~3 fold decrease in the net protrusion velocity of Pfn1-deficient cells (Fig. 13E). Note that similar to MDA-231 cells, the average speed of Pfn1-deficient HMEC is also reduced by 40% when Lpd expression is suppressed (Fig. 13F).

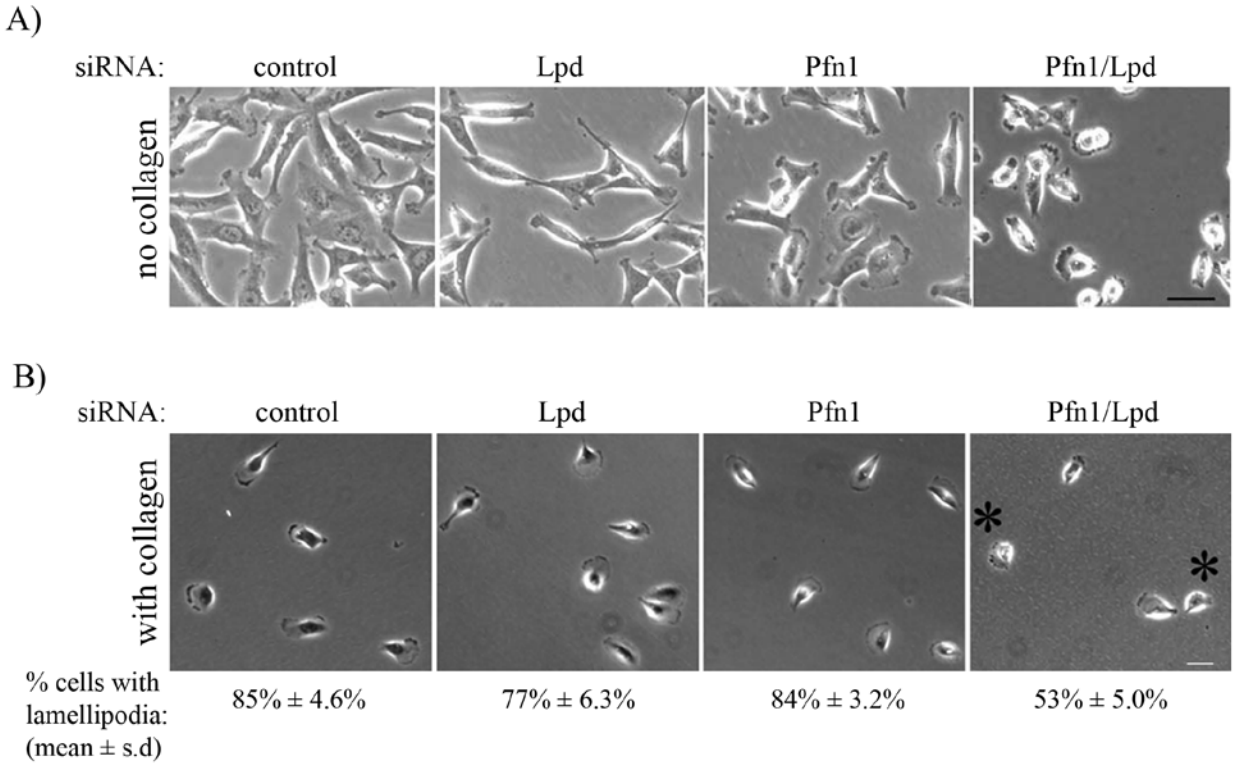
A)
siRNA:
control
Lpd
Pfn1
Pfn1/Lpd
no collagen
B)
siRNA:
control
Lpd
Pfn1
Pfn1/Lpd
with collagen
% cells with lamellipodia: (mean ± s.d)
85% ± 4.6%
77% ± 6.3%
84% ± 3.2%
53% ± 5.0%

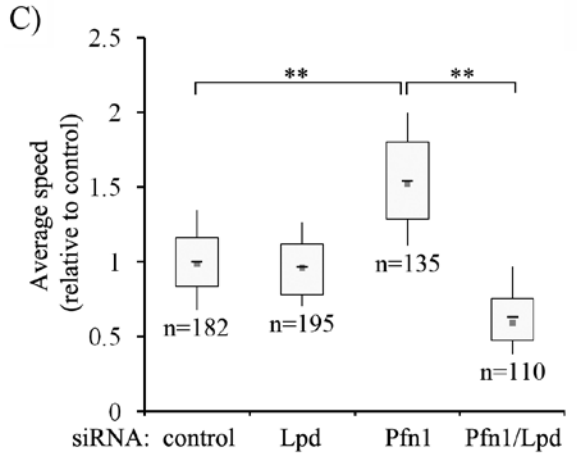
C)
Average speed (relative to control)
2.5
2
1.5
1
0.5
0
**
**
n=182
n=195
n=135
n=110
siRNA: control
Lpd
Pfn1
Pfn1/Lpd

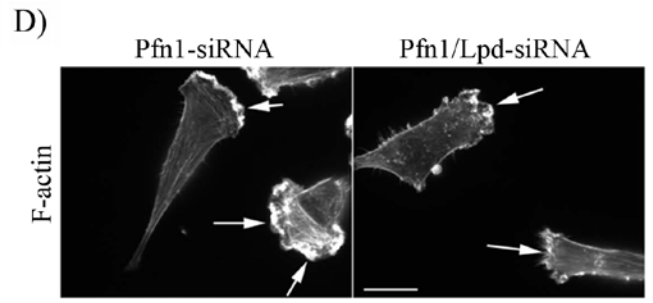
D)
Pfn1-siRNA
Pfn1/Lpd-siRNA
F-actin

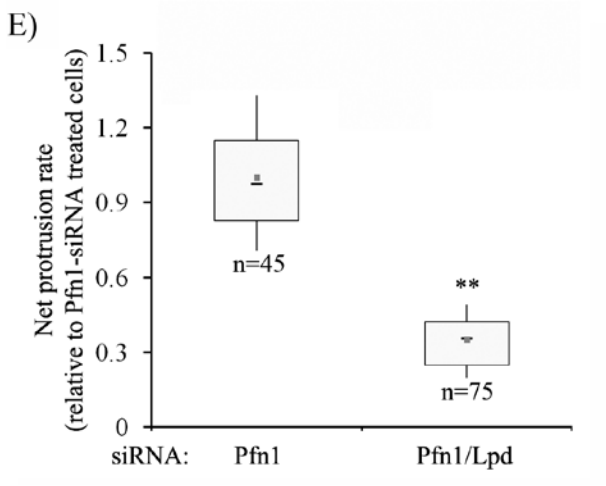
E)
Net protrusion rate (relative to Pfn1-siRNA treated cells)
1.5
1.2
0.9
0.6
0.3
0
n=45
**
n=75
siRNA:
Pfn1
Pfn1/Lpd

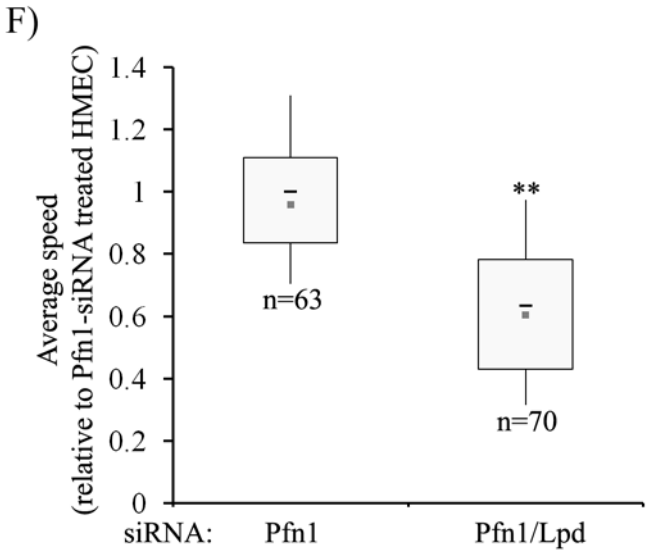

Figure 13: Lpd plays a key role in the hypermotile response of Pfn1-deficient MDA-231 cells. **A)** Phase-contrast micrographs of MDA-231 cells plated on tissue culture substrate without ECM coating following transfection of various siRNAs indicated in the figure (scale bar - 50μm). **B)** Phase contrast micrographs of MDA-231 cells plated on collagen-coated tissue-culture substrate show defect in lamellipodia formation (marked by asterisks) only in cells with co-suppression of Lpd and Pfn1 expression (mean ± sd values for % of cells with lamellipodia formation for the various siRNA-treated groups are indicated below; data summarized from 2-3 independent expts with >125 cells analyzed in each group). Scale bar - 50μm. **C)** A box and whisker plot comparing the average speed of migration of control and Pfn1-siRNA treated MDA-231 cells with or without limiting Lpd expression. **D)** Phalloidin staining reveals marked reduction in F-actin content at the leading edge (arrows) in Pfn1-depleted cells when Lpd expression is downregulated (scale bar - 20μm). **E)** A box and whisker plot comparing the net protrusion rate of Pfn1-depleted MDA-231 cells with or without Lpd suppression. **F)** A box and whisker plot comparing the average migration speed of Pfn1-depleted HMEC with or without Lpd suppression (n' indicates the number of cells analyzed in each treatment group and ** denotes $p<0.01$).

5.1.2 Pfn1 exerts its inhibitory action on breast cancer cell motility predominantly through its phosphoinositide interaction

In order to obtain insight on how reduced Pfn1 level increases breast cancer cell motility, we first asked which among the three major ligand interactions of Pfn1 (i.e actin, polyproline or phosphoinositide) predominantly inhibits breast cancer cell migration. To address this question, we stably expressed either GFP-Pfn1 (fully functional form of Pfn1) or various previously characterized ligand-binding deficient mutants of Pfn1 in MDA-231 (a highly aggressive breast cancer cell line which expresses significantly lower Pfn1 compared to normal HMEC and display dramatically enhanced motility upon Pfn1 depletion [Zou et al., 2007; Bae et al., 2009]) cells. Note that fusing GFP to the N-terminus of Pfn1 as done in our case preserves the biochemical functions and cellular localization of the fusion protein similar to that of endogenous Pfn1 [Wittenmayer et al., 2000]. The various GFP-tagged Pfn1 mutants we expressed are: H119E-Pfn1 as actin-binding mutant (it has a ~30 fold reduction in actin-binding compared to wild-type Pfn1 but retains normal polyproline binding), H133S-Pfn1 as polyproline-binding mutant (it has normal actin and $PI(4,5)P_2$-binding but 50-fold less polyproline-binding compared to wild-type) and R88L-Pfn1 as PPI-binding mutant (it has normal polyproline binding but is substantially defective in $PI(4,5)P_2$ binding (less than 30% of the wild-type value)) [Zou et al., 2007; Suetsugu et al., 1998; Sohn et al., 1995; Wittenmayer et al., 2004; Ezezika et al., 2009; Lu et al., 2001; Richer et al., 2008]. Note that like all PPI-binding deficient mutants discovered to date, R88L-Pfn1 mutant also has ~2-3-fold deficiency in actin-binding because of partial structural overlap between PPI and actin binding sites of Pfn1 [Sohn et al., 1995; Wittenmayer et al., 2004]. We engineered all of these Pfn1 constructs to be resistant to Pfn1-siRNA treatment by introducing additional silent mutations in the siRNA-targeting region; this strategy enabled us to

express these various constructs in MDA-231 cells in the background of strongly suppressed endogenous Pfn1 expression achieved via Pfn1-siRNA treatment. As a control, we used our previously generated stable GFP expresser of MDA-231 cells [Zou et al., 2007] which were transfected with either non-targeting control or Pfn1-siRNA. The immunoblots in the inset of Figure 14A demonstrate that i) we are able to express various GFP-Pfn1 constructs in the background of a close to 100% suppression of endogenous Pfn1 expression, and ii) the relative expression of these Pfn1 constructs are similar between the different sublines of MDA-231 cells. We estimated the level of exogenous Pfn1 to be approximately 70-80% of that of endogenous Pfn1 (Fig. 14B). Sub-cellular fractionation analyses showed that GFP-Pfn1 is more abundantly localized in cytosol than at the membrane, as in a previously report in other cell types [Hartwig et al., 1989] (Fig. 14C). Note that similar to endogenous Pfn1, GFP-Pfn1 is also localized in nucleus to a certain extent (nuclear localization is strongest for H119E-Pfn1 mutant) which was not analyzed in the fractionation experiment. As expected from its reduced binding to PPI, membrane content of R88L-Pfn1 mutant was found to be significantly less compared to the other three variants of Pfn1 (Fig. 14D).

When we compared the relative speed of migration of these various cell lines by time-lapse imaging, we found that that the average speed of control GFP expressers increases by ~2 fold when Pfn1 expression is silenced (this is consistent with our previous observation on parental MDA-231 cells [Bae et al., 2009]), and the hypermotile phenotype of Pfn1-deficient cells can be completely rescued by GFP-Pfn1. Among the various Pfn1 mutants, H119E-Pfn1 and H133S-Pfn1 rescue the hypermotile response of Pfn1-silenced cells by nearly 70% and 85%, respectively; but R88L-Pfn1 mutant fails to rescue the hypermotile phenotype (in fact, there was no significant difference in the average speed between R88L-Pfn1 re-expressers and control GFP

cells in suppressed endogenous Pfn1 background) (Fig. 14E). Even though R88L substitution decreases actin-binding of Pfn1 by 2-3 fold in addition to causing a major defect in its PPI binding, given that expression of H119E-Pfn1 (a much more potent actin-binding mutant which has a ~30-fold reduction in actin-binding compared to wild-type Pfn1) is able to reduce the speed of Pfn1-deficient cells by 70%, our data strongly suggests that the hypermotile response of the R88L mutant is not related to loss of Pfn1's interaction with actin. Also, since the average speed of GFP-Pfn1-H119E expressers is somewhat higher than that of GFP-Pfn1 expressers, this rules out an alternative explanation of our motility data based on mutual exclusion of actin and PPI interaction of Pfn1 i.e. "R88L-Pfn1 being less sequestered at the membrane enhances cell motility through more frequent association with actin". Therefore, hypermotile response of R88L-Pfn1 mutant is attributed to loss of PPI interaction of Pfn1.

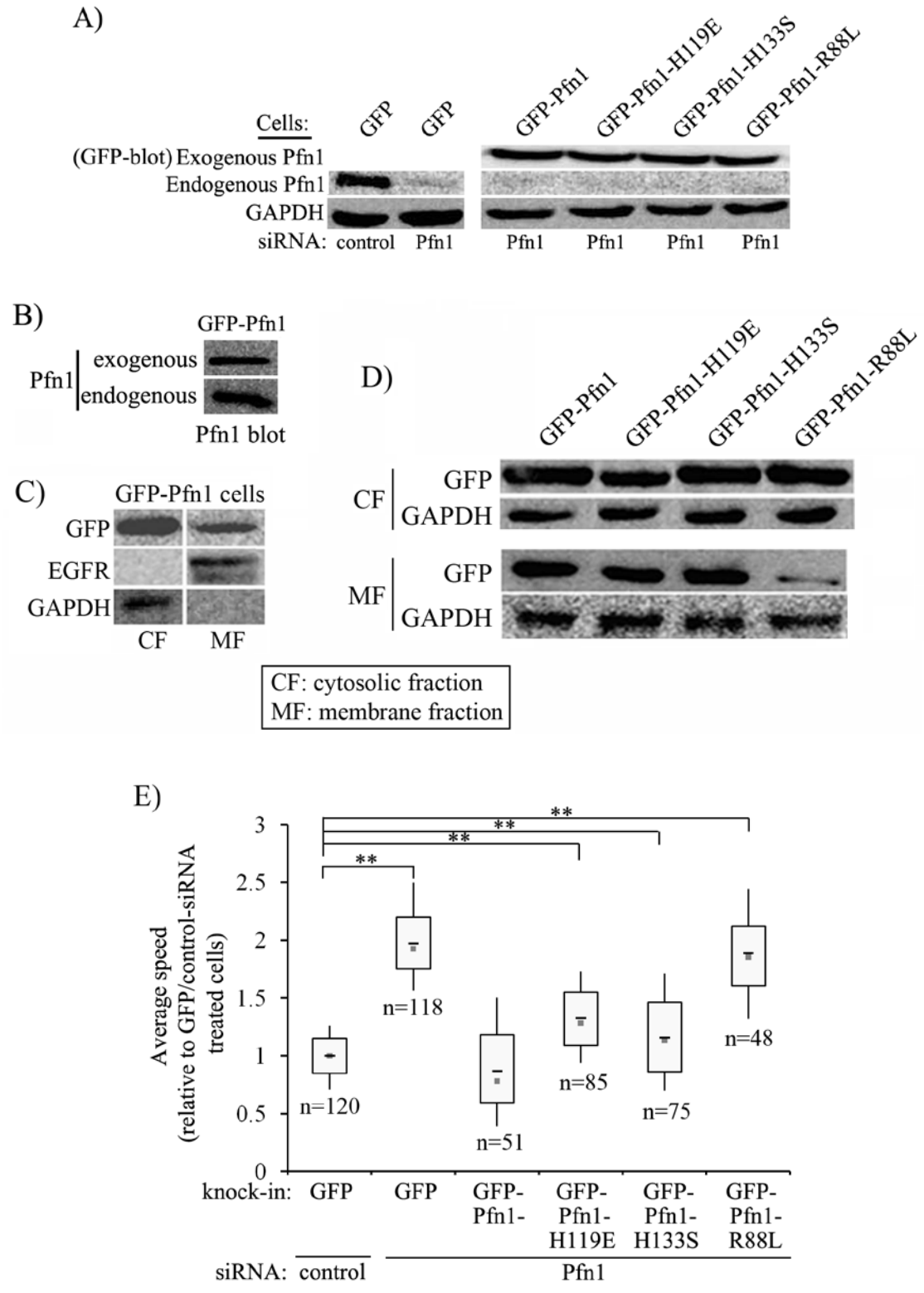

Figure 14: Pfn1 inhibits MDA-231 breast cancer motility predominantly through its PPI interaction. A) Pfn1 and GFP immunnoblots show the endogenous and exogenous Pfn1 contents for various stable sublines of MDA-231 cells under different siRNA treated conditions (Pfn1 and

of GFP expressers that are transfected with control siRNA serves as a standard for comparison; GAPDH blot - loading control). **B)** Pfn1 immunoblot of GFP-Pfn1 expressers shows relative levels of endogenous and exogenous Pfn1.**C-D)** GFP-immunoblot of equal amounts of protein from cytosolic (CF) and membrane (MF) fractions of GFP-Pfn1 rescue expressers, shows relative abundance of GFP-Pfn1 in cytosol and membrane (*panel C*). GFP immunoblots of CF and MF show the relative cytosolic and membrane contents of GFP-Pfn1 and its various mutants in the respective sublines (*panel D* - note that the exposure time for MF blot shown in panel D is much higher than the corresponding CF blot to reveal the weak MF band for R88L-Pfn1). EGFR and GAPDH blots serve as the markers for MF and CF samples, respectively. **E)** A box and whisker plot summarizing the effect of abolishing various ligand interactions of Pfn1 on the average speed of migration of MDA-231 cells. ‘‘N’ indicates the number of cells analyzed in each group pooled at least 3 independent experiments analyzed (**: $p<0.01$).

We previously showed that Pfn1 depletion results in slower but more stable (less prone to withdrawal) membrane protrusion thereby increasing the net protrusion velocity of parental MDA-231 cells [Bae et al., 2009]. Importantly, the cells analyzed in each of these six groups form normal appearing lamellipodia in motility experiments (Fig 15A); however, kymography analyses of membrane protrusion showed that the average net protrusion velocity of R88L-Pfn1 mutant cells (=1.15 μm/min) is significantly higher than any of the other rescue cell lines and very similar to the value obtained for Pfn1-depleted cells (=1 μm/min) (Fig. 15B-C). Overall, our findings indicate that Pfn1 inhibits MDA-231 cell migration predominantly through its PPI interaction. Note that we did not find any significant difference in either actin expression or the overall cellular F-actin level between GFP-Pfn1 (full rescue) and GFP-Pfn1-R88L rescue expressers (Fig 16); therefore, a striking difference in the protrusion kinetics between the two cell lines suggests that F-actin dynamics and/or protrusion/adhesion coupling at the leading edge are likely to altered by the PPI mutation of Pfn1.

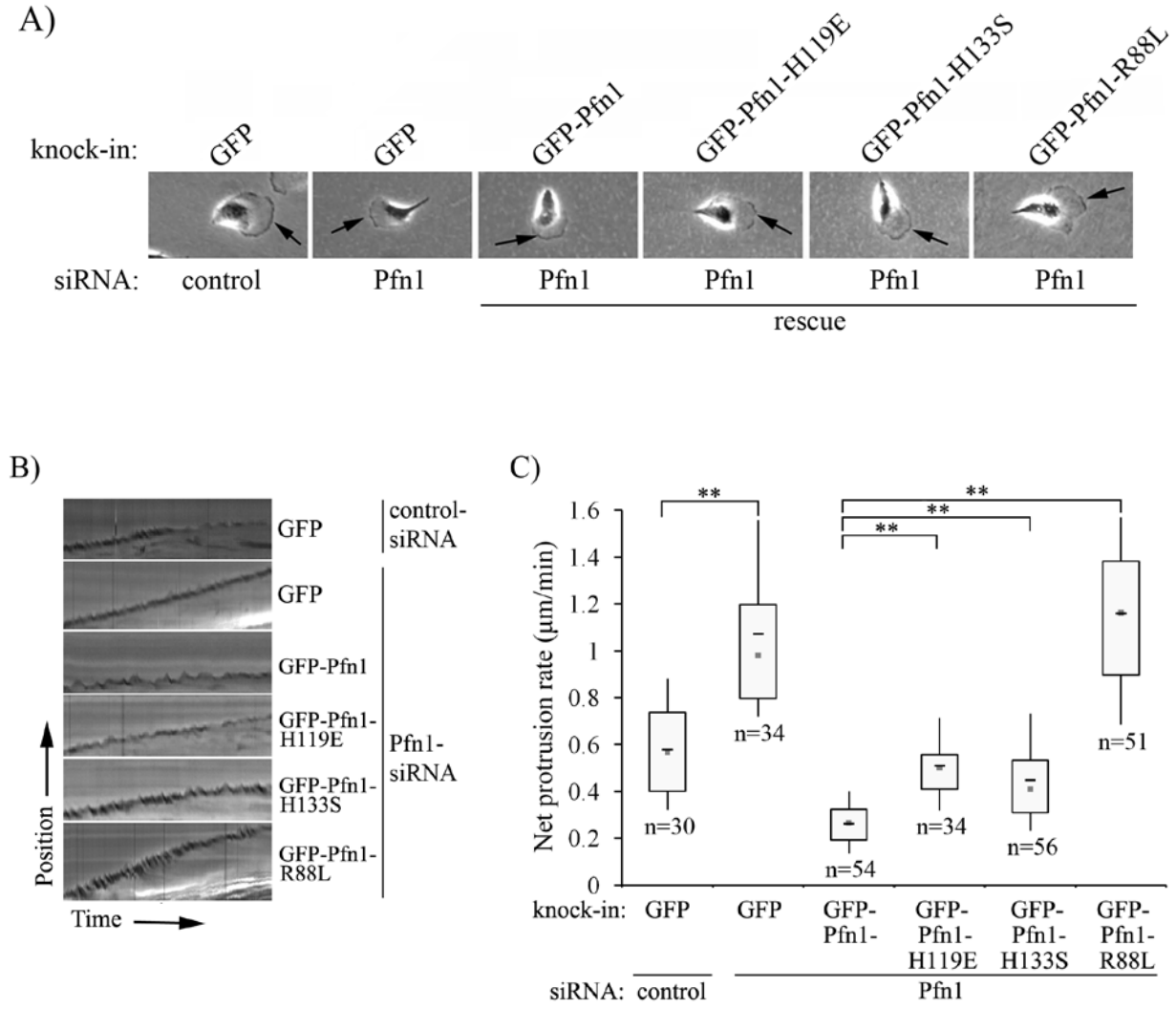

Figure 15: Protrusion dynamics of various sublines of MDA-231 cells. A) Phase-contrast micrographs of migrating cells show normal appearing lamellipodia (arrows) formed by the various experimental groups of MDA-231 cells. **B-C)** A set of representative kymographs of protruding membrane (*panel B*) and a box and whisker plot comparing the net protrusion rate (*panel C*) between the different experimental groups of cells measured from kymography assay (‘‘N’ indicates the number of cells analyzed in each group pooled at least 3 independent experiments analyzed (**: $p<0.01$).

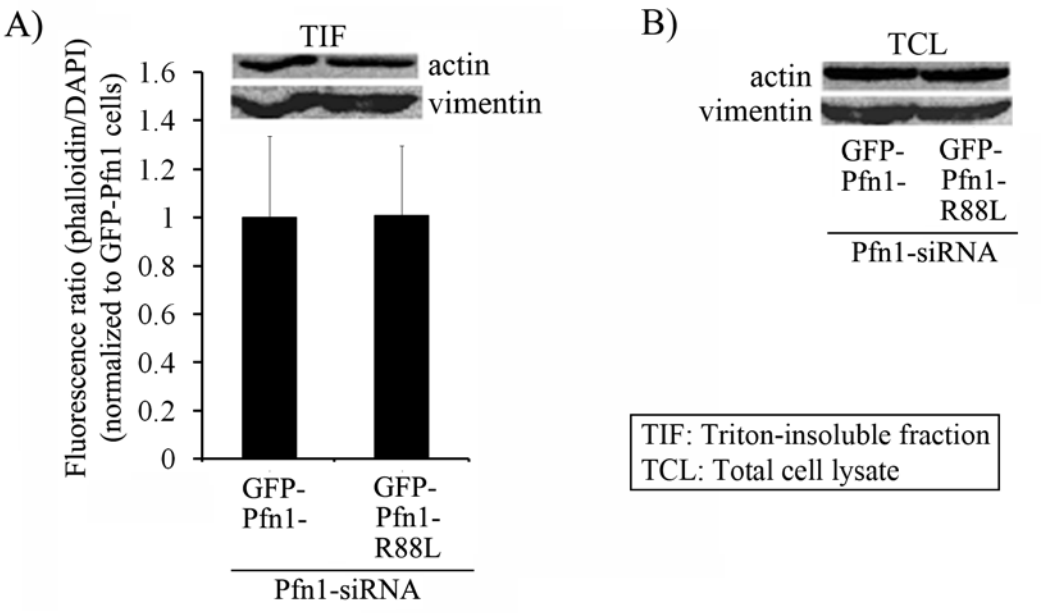

Figure 16: A) A comparison of total cellular F-actin content between GFP-Pfn1 and GFP-Pfn1-R88L rescue sublines of MDA-231 cells as measured by either fluorescence assay (data summarized from 3 independent experiments) or immunoblot-based detection of actin in the triton-insoluble fraction of cell lysate (inset of panel A). **B)** Relative actin expression between the two cell lines. Vimentin blots serve as the loading controls.

5.1.3 Pfn1 inhibits breast cancer cell motility by negatively regulating Lpd targeting to the leading edge through its phosphoinositide interaction

We previously demonstrated that lowering Pfn1 expression in normal HMEC and MDA-231 cells enhances lamellipodial targeting but not the total expression level of VASP (a protein known to localize at focal adhesion, distal rim of lamellipodia, filopodia and actin stress-fibers [Rottner et al., 1999]) and that hypermotile response of Pfn1-deficient MDA-231 cells is Ena/VASP-dependent [Bae et al., 2009]. Membrane targeting of Ena/VASP proteins also positively correlates with protrusion velocity and overall speed of migration of fish scale keratocytes, another rapidly migrating cell type [Lacayo et al., 2007]. Given our present data with MDA-231 cells showing similar overall speed and net protrusion velocity between R88L-Pfn1 rescue expressers and Pfn1 knockdown cells, we asked whether PPI-interaction of Pfn1 plays any role in regulating VASP targeting to the leading edge. Indeed, immunostaining of our various rescue cell lines showed that VASP-rich lamellipodial rim, a feature of Pfn1-depleted cells, is mimicked predominantly in R88L-Pfn1 expressers (Fig. 17A) thus demonstrating that PPI interaction of Pfn1 inhibits targeting of VASP to the leading edge in MDA-231 cells. Similar to our finding related to VASP, we found that among the various rescue sublines of MDA-231 cells, only R88L-Pfn1 expressers display a very strong Lpd-staining at the lamellipodial tip similar to what is seen in Pfn1-knockdown cells (Fig. 17B). Note that the same R88L-Pfn1 expressers, when treated with control-siRNA (mimics a moderate overexpression setting), neither exhibit Lpd-rich lamellipodial tip (Fig. 17C) nor produce a hypermotile phenotype when compared to control GFP expressers (Fig. 17D). Similarly, in a transient-transfection based assay, the difference in the average speed between GFP and GFP-Pfn1-R88L overexpresser was found to be only 10% (not statistically significant) which further confirmed the results from stable

expressers in control siRNA-based setting. Since endogenous Pfn1, when present in R88L-Pfn1 expressers, should still be able to interact with the membrane, these overexpression-based results further establish that the phenotypes exhibited by R88L-Pfn1 mutant in a rescue situation (i.e in the absence of endogenous Pfn1 expression) are specifically due to the loss of PPI interaction of Pfn1 and not secondary to other changes induced by the mutant. In summary, our findings thus far demonstrate that Pfn1 negatively regulates membrane targeting of Lpd and VASP at the leading edge through its PPI interaction.

Since R88L-Pfn1 rescue expressers phenocopy Pfn1-knockdown cells in terms of comparable hypermotile response, net protrusion velocity, formation of Lpd/VASP-rich lamellipodial rim, we next asked whether VASP and Lpd contribute to the hypermotile response of this rescue cell line. To assess the contribution of VASP, we expressed mCherry-tagged FP4-mito, a construct that sequesters all members of Ena/VASP proteins to the mitochondria thereby inhibiting their function (as a control, cells were transfected with mCherry-tagged AP4-mito, a similar structured construct that also targets to mitochondria but fails to bind to Ena/VASP proteins). Figure 17E shows Ena/VASP inhibition by mCherry-FP4-mito results in a ~ 3.2-fold reduction in the average speed of migration of R88L-Pfn1 expressers. This is specific to Ena/VASP inhibition since expression of mCherry-AP4-mito (control construct) did not show any significant change in motility when compared to untransfected (mCherry-negative) cells. Likewise, motility of R88L-Pfn1 mutant cells also showed strong dependence on Lpd availability since limiting Lpd expression by siRNA treatment led to a 2-fold decrease in cell speed (Fig. 17F - the immunoblot in the inset confirms Lpd suppression by siRNA treatment). A stronger inhibitory effect of VASP inhibition (~3.2 fold) compared to Lpd depletion (~2 fold) on motility of R88LPfn1 mutant cells was not surprising given that we failed to achieve a complete

knockdown of Lpd expression by siRNA treatment whereas we have seen that FP4-mito construct is highly effective in sequestering all of the detectable cellular pool of VASP to the mitochondria in MDA-231 [Bae et al., 2009]. Given Lpd's requirement for VASP recruitment to the leading edge, our overall data indicate that PPI interaction of Pfn1 confers the major inhibitory effect of Pfn1 on breast cancer cell motility secondary to the availability of Lpd and in turn VASP at the leading edge.

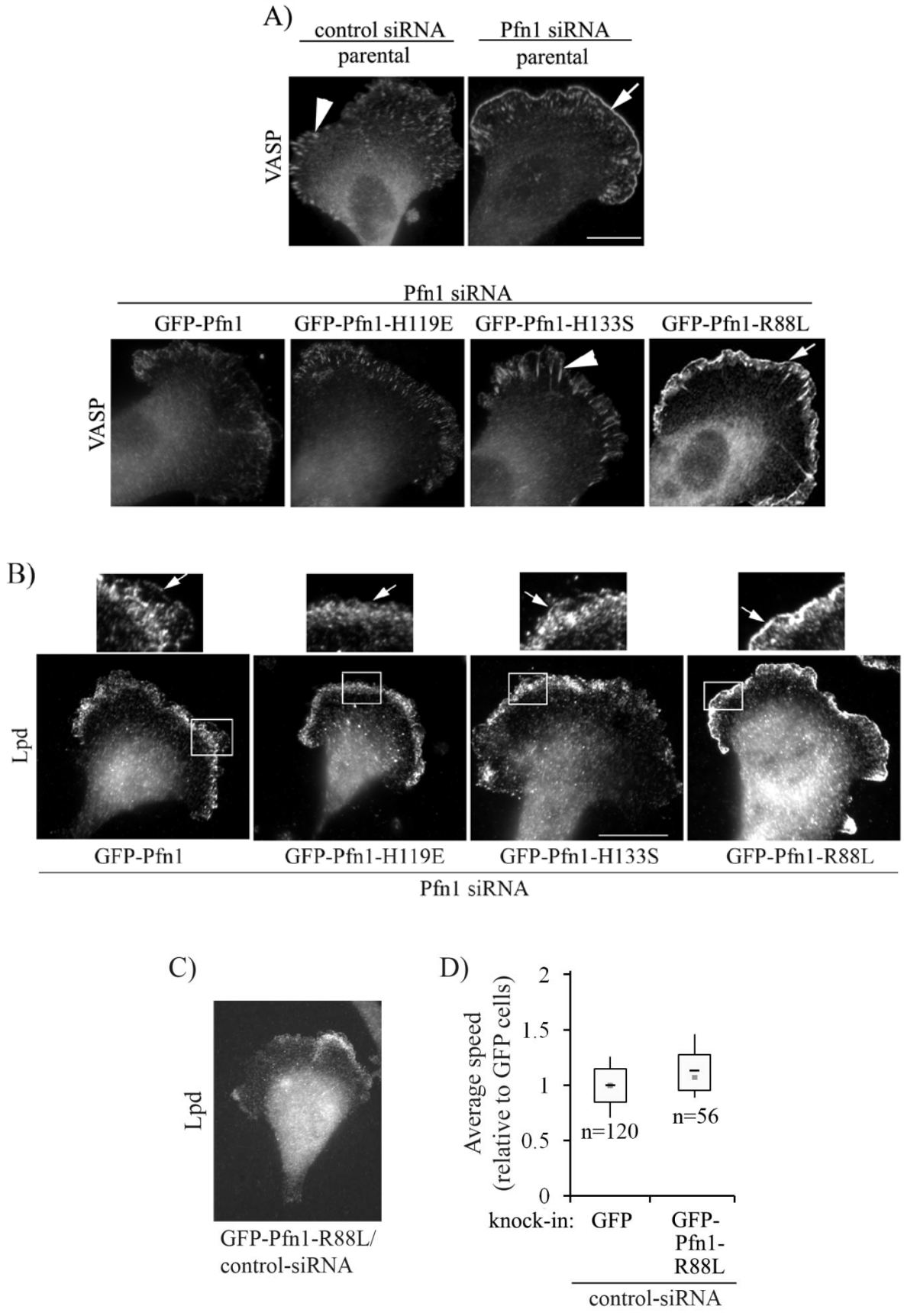
A)
control siRNA
parental
Pfn1 siRNA
parental
VASP
Pfn1 siRNA
GFP-Pfn1
GFP-Pfn1-H119E
GFP-Pfn1-H133S
GFP-Pfn1-R88L
VASP
B)
Lpd
GFP-Pfn1
GFP-Pfn1-H119E
GFP-Pfn1-H133S
GFP-Pfn1-R88L
Pfn1 siRNA
C)
Lpd
GFP-Pfn1-R88L/
control-siRNA
D)
Average speed
(relative to GFP cells)
2
1.5
1
0.5
0
n=120
n=56
knock-in:
GFP
GFP-
Pfn1-
R88L
control-siRNA

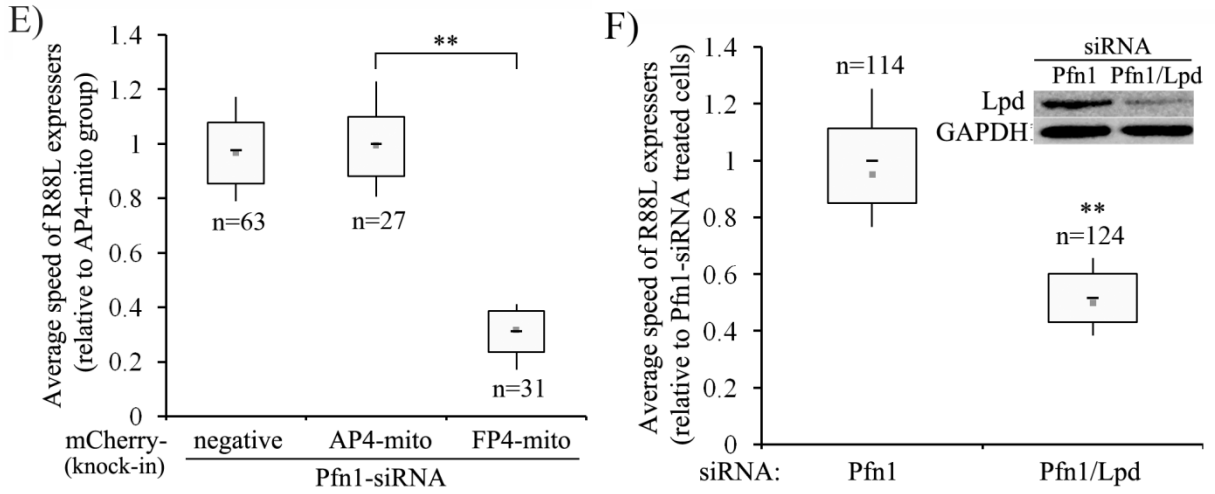

Figure 17: Pfn1 limits VASP and Lpd distribution at the leading edge through its PPI interaction. A) Immunostaining show that only R88L-Pfn1 expressers show strong VASP localization at the leading edge (arrow) similar to Pfn1-depleted cells (arrowheads shows the characteristic focal adhesion localization of VASP). **B)** Lpd staining of various rescue expressers of MDA-231 cells shows strongest Lpd-staining at the lamellipodial tip in R88L-Pfn1 rescue subline. Magnified forms of the insets (outlined by the boxes) are displayed above. **C)** Lpd immunostaining of GFP-Pfn1-R88L expressers of MDA-231 cells following control siRNA transfection. **D)** A bar graph summarizing the average speed of migration of GFP and GFP-Pfn1-R88L expressers following control siRNA transfection. 'N' indicates the number of cells analyzed for each group of cells pooled from 2 independent experiments. **E)** A box and whisker plot demonstrates that Ena/VASP sequestration by mCherry-FP4-mito dramatically inhibits motility of R88L-Pfn1 mutant expressers. Untransfected or m-Cherry-AP4 transfected cells serve as the two control groups in Ena/VASP sequestration experiments. "N" indicates the number of cells analyzed for each experimental group pooled from at least 3 independent experiments (**: $p<0.01$). **F)** A box and whisker plot comparing the average speed of migration of R88L-Pfn1 expressers with or without Lpd suppression (the immunoblot in the inset shows strong suppression of Lpd expression; GAPDH blot - loading control). For all experiments, ''N' indicates the number of cells analyzed in each group pooled from at least 3 independent experiments (**: $p<0.01$). The scale bar in all images represents 20 µm.

5.1.4 Loss of Pfn1 expression enhances PI(3,4)P_2 presentation at the leading edge

In vitro studies showed that PH domain of Lpd binds specifically to PI(3,4)P_2 (this does not bind to any other 3'-phosphorylated-PPI [D3-PPI] such as PI3P or PI(3,4,5)P_3) [Krause et al., 2004]. A recent study further demonstrates that enteropathogenic bacteria generates PI(3,4)P_2-rich platform at the host-cell membrane to recruit Lpd [Smith et al., 2010] thus suggesting that Lpd docks to plasma membrane via its binding primarily to PI(3,4)P_2. Activation of various receptor tyrosine kinases such as EGFR (EGF-receptor) and PDGFR (PDGF-receptor) stimulate PI3-kinase [PI3K] activity and generate PI(3,4,5)P_3, which when dephosphorylated by 5'-phosphatases (such as SHIP2) lead to the production of PI(3,4)P_2. To initially confirm the role of D3-PPI (such as PI(3,4)P_2) in VASP and Lpd targeting to leading edge in our case, we subjected Pfn1-deficient MDA-231 cells (either without or with R88L-Pfn1 rescue) to acute PDGF stimulation either in the presence of LY294002 (a pharmacological inhibitor of PI3K that reduces both PI(3,4)P_2 and PI(3,4,5)P_3) or DMSO (diluent control). We found that Lpd localization at the leading edge in both Pfn1 knockdown cells and R88L-Pfn1 rescue expressers is dramatically reduced in response to LY294002 treatment (Fig. 18A-B - diluent control DMSO preserves strong VASP and Lpd localization at the leading edge as expected). Consistent with these results, overexpression of either GFP-PTEN (phosphatase and tensin homolog deleted on chromosome 10 - a dual lipid-protein phosphatase that dephosphorylates D3-PPIs and reduces their level) or GFP-PH-AKT (a reporter that binds to D3-PPI including PI(3,4)P_2 and should therefore act as a competitor for other ligands, such as Lpd, for binding to PPI) also completely abolishes the strong Lpd distribution at the leading edge in Pfn1-depleted cells (Fig. 18C - as a negative control, expression of GFP maintains the characteristic Lpd-rich lamellipodial rim as expected). Based on these data demonstrating the sensitivity of membrane targeting of Lpd to

D3-PPI perturbation, we speculated that loss of Pfn1 expression might enhance Lpd-targeting to the lamellipodial tip through influencing $PI(3,4)P_2$ content at the membrane of the leading edge. To test this, we examined $PI(3,4)P_2$ distribution at the leading edge between control and Pfn1-siRNA treated MDA-231 cells either in basal (serum-starved) or various growth factor (EGF, PDGF) stimulated conditions by immunostaining. Figures 18D-E demonstrate that cells under either siRNA transfected condition exhibit increased $PI(3,4)P_2$ content at the leading edge in response to acute EGF/PDGF stimulation; however, Pfn1-depleted cells have significantly higher $PI(3,4)P_2$ accumulation at the leading edge compared control cells in response to these various growth-factor stimulated conditions. Stronger $PI(3,4)P_2$ presentation at the leading edge in Pfn1-deficient cells is clearly consistent with enhanced Lpd targeting to the lamellipodial tip in these cells.

It is known that EGF signaling, in particular, plays a key role in breast cancer cell migration/invasion in vitro and in vivo [Goswami et al., 2005; Wyckoff et al., 2004; Xue et al., 2006]. We therefore asked whether loss of Pfn1 expression alters the expression and/or activation of EGFR in MDA-231 cells. Immunoblot data in Figure 18F show that EGF-induced phosphorylation of EGFR at its Y1164 residue (a measure of EGFR activation) and the overall expression level of EGFR are unaffected by silencing of Pfn1. Similarly, the expression level of PDGFRβ and PDGF-induced tyrosine phosphorylation of PDGFR (correlates with its activation) were found to be similar between control and Pfn1-depleted cells (Fig. 18G-H). Finally, EGF-dependent phosphorylation of AKT, a downstream signaling that involves PI3K-mediated generation of $PI(3,4,5)P_3$, was also found to be comparable between control and Pfn1-siRNA treated cells (Fig 16I). These results indicate that Pfn1-depletion induced increase in $PI(3,4)P_2$ accumulation at the leading edge is not due to altered RTK activation.

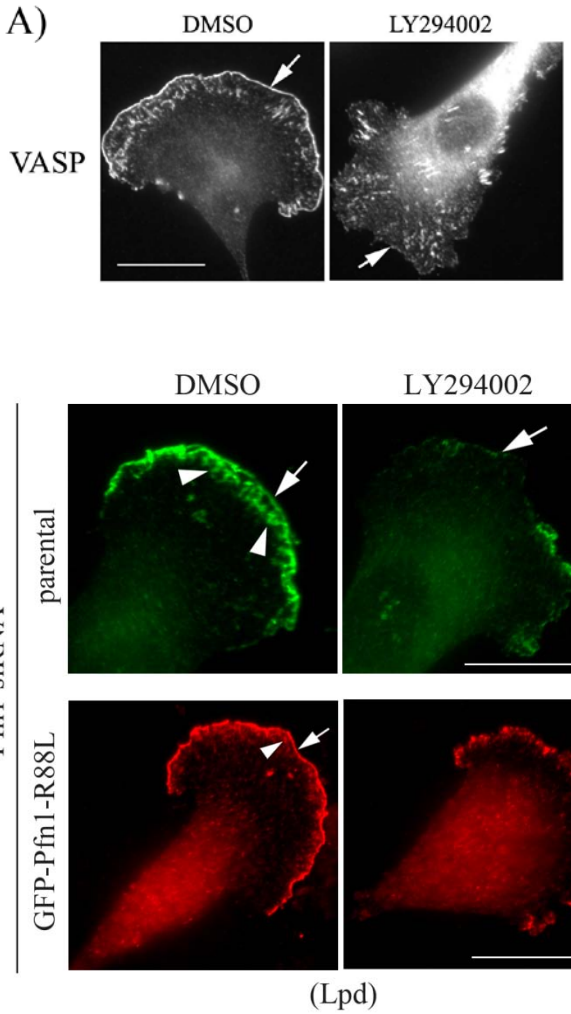
A)
DMSO
LY294002
VASP
B)
DMSO
LY294002
Pfn1-siRNA
parental
GFP-Pfn1-R88L
(Lpd)
C)
Expression:
GFP
GFP-PTEN
GFP-PH-AKT
Pfn1-siRNA
Lpd
GFP

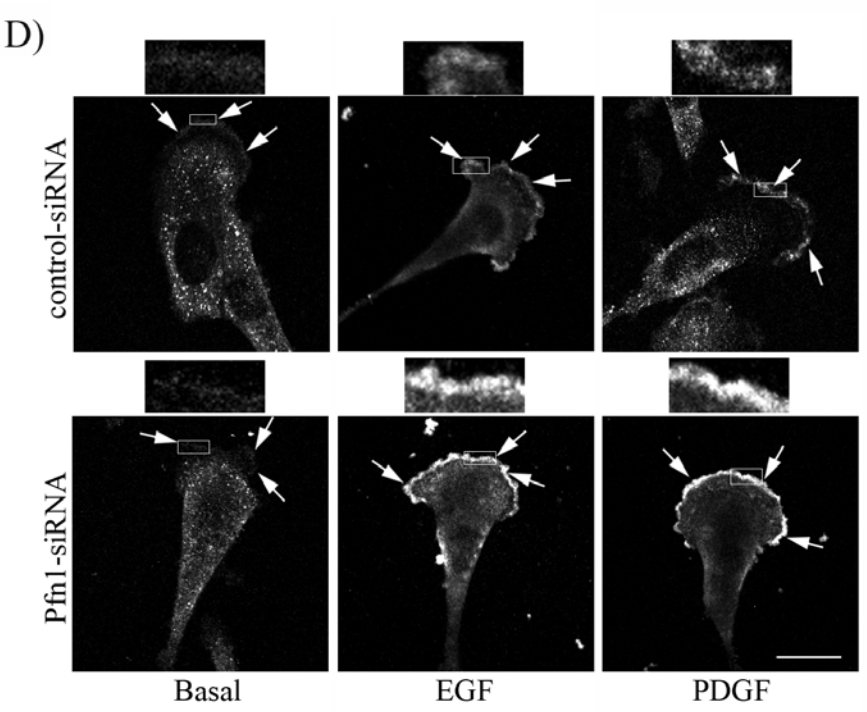
D)
control-siRNA
Pfn1-siRNA
Basal
EGF
PDGF

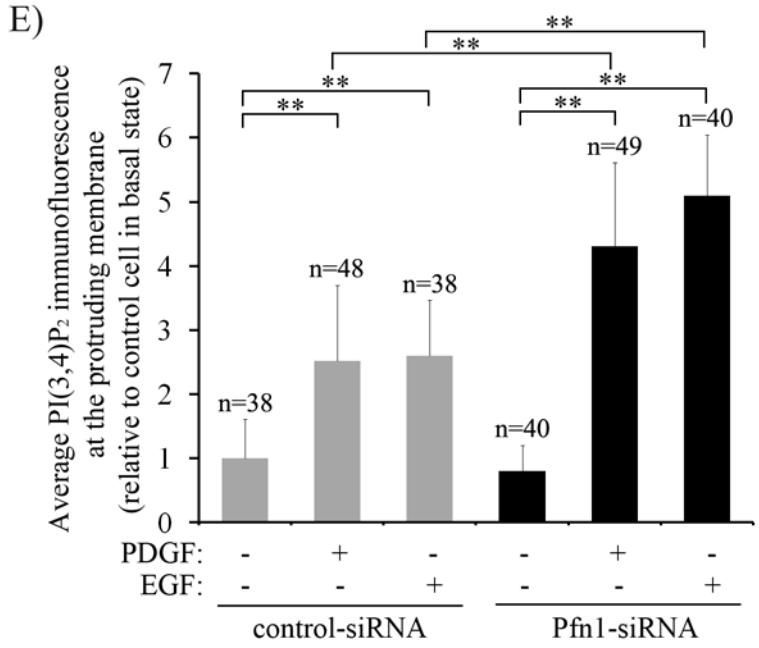
E)
Average PI(3,4)P2 immunofluorescence at the protruding membrane (relative to control cell in basal state)
0
1
2
3
4
5
6
7
**
**
**
**
**
**
n=38
n=48
n=38
n=40
n=49
n=40
PDGF: - + - - + -
EGF: - - + - - +
control-siRNA
Pfn1-siRNA

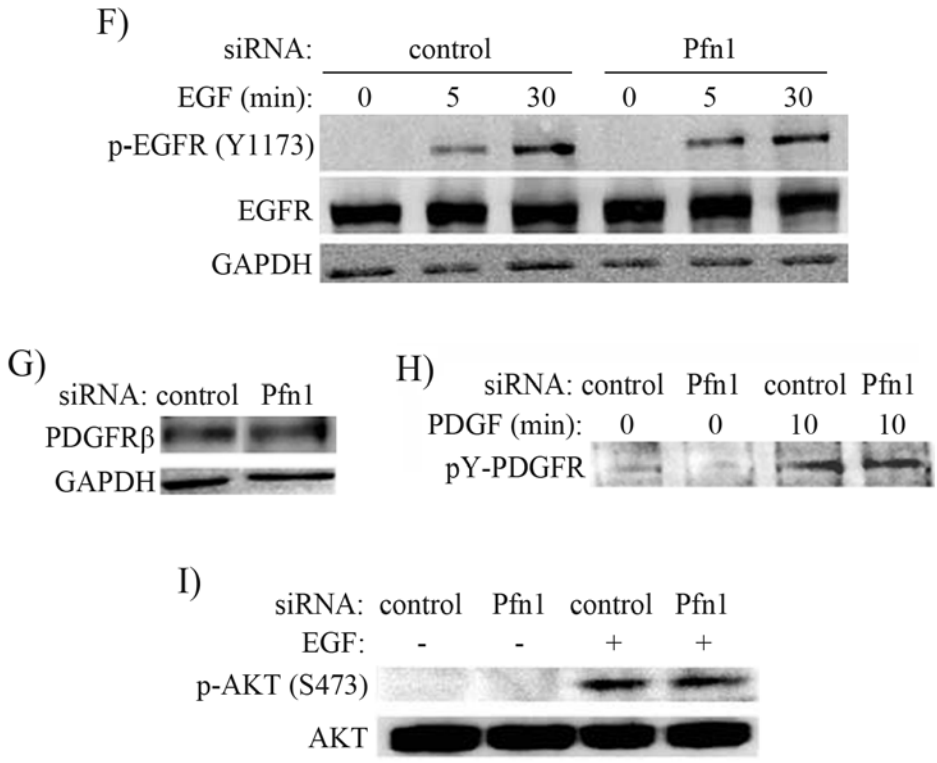

Figure 18: Loss of Pfn1 expression enhances PI(3,4)P_2 accumulation at the leading edge in MDA-231 cells. A) LY294002 treatment dramatically delocalizes VASP from the leading edge (arrows), while DMSO (diluent control) treated cells show strong lamellipodial distribution of VASP as expected. **B)** PI3K inhibition by 30 min LY294002 treatment delocalizes Lpd from the leading edge (arrows) in PDGF-treated Pfn1-knockdown MDA-231 cells without or with R88L-Pfn1 rescue (DMSO - vehicle control; arrowhead shows Lpd in membrane ruffles). **C)** Expression of either GFP-PTEN or GFP-PH-AKT but not GFP (control) delocalizes Lpd from the leading edge (arrow) in Pfn1-deficient cells. **D-E)** Representative confocal images (*panel D*; inset shows magnified images of regions outlined by the boxes) and bar graph summarizing relative intensity (*panel E*) of PI(3,4)P_2 immunostaining at the leading edge in control and Pfn1-siRNA treated MDA-231 cells either in basal (serum-starved) or following 30 minutes of EGF and PDGF stimulation (arrows show leading edge). 'N' indicates number of cells analyzed in each group (**: $p<0.01$). **F)** Phosphorylation of EGFR at Y1173 residue and total EGFR level at different time-points after EGF stimulation in control and Pfn1-siRNA treated cells (GAPDH blot - loading control). **G)** Relative PDGFR-β expression level between control and Pfn1 siRNA treated MDA-231 cells (GAPDH blot – loading control). **H)** Phosphotyrosine (pY) immunoblot showing PDGF-induced phosphorylation of PDGFR in control and Pfn1 siRNA treated cells. **I)** Effect of silencing Pfn1 expression on the level of phospho-AKT (S473) 10 min after EGF stimulation (AKT blot - loading control). The scale bar in all images represents 20 μm.

5.2 DISCUSSION

A context-dependent role for Pfn1 in cell migration is becoming increasingly evident based on differential response of whole cell motility to Pfn1 depletion depending on the cell type. While certain types of normal cells (example: human vascular endothelial cells) show impaired motility upon loss of Pfn1 function, the opposite occurs with adenocarcinoma (breast, hepatic) cells and even some normal cells such as HMEC. Conventional principle of action of Pfn1 through its actin and polyproline interactions facilitating membrane protrusion during cell migration cannot explain the hypermotile response of breast cancer cells and HMEC enabled in the absence of Pfn1. We here describe a novel mechanism of Pfn1-dependent regulation of breast cancer cell migration involving its PPI interaction and using Lpd, a PPI-binding Ena/VASP ligand, as a mediator.

Using a knockdown-knockin strategy, we demonstrated that two important phenotypic characteristics of MDA-231 cells associated with Pfn1-depletion including hypermotile behavior and strong distribution of Lpd/VASP at the lamellipodial tip are completely abolished by GFP-Pfn1 re-expression therefore confirming the functional rescuing ability of GFP-Pfn1. Among the three mutants of Pfn1, only the PPI binding-deficient form (R88L) fails to rescue these phenotypes. We found a striking similarity between R88L-Pfn1 re-expressers and Pfn1-deficient cells in terms of their motility speed, average velocity of protrusion and Lpd/VASP distribution at the lamellipodial tip and these data provide a direct evidence of Pfn1's negative regulation of Lpd/VASP localization at the leading edge and motility of breast cancer cells predominantly through its PPI interaction. Even though the effect of Lpd knockdown on whole cell motility has not been previously examined, impaired lamellipodia formation and slower membrane protrusion in fibroblasts resulting from Lpd knockdown suggest that Lpd is an important regulator of

lamellipodial dynamics [Krause et al., 2004]. The same study also showed that Lpd overexpression leads to faster membrane protrusion in fibroblasts which can be suppressed by Ena/VASP inhibition further indicating that Ena/VASP plays a key role in Lpd's regulation of membrane dynamics at the leading edge. Ena/VASP proteins bind to and promote elongation of barbed ends of actin filaments [Barzik et al., 2005; Pasic et al., 2008]. This has been proposed to be the mechanism underlying Ena/VASP-driven actin assembly at the leading edge and membrane protrusion. We previously demonstrated Ena/VASP's involvement in the hypermotile response of MDA-231 cells induced by Pfn1 downregulation [Bae et al., 2009]. The present study showed Lpd's role in VASP recruitment to the lamellipodial tip, regulation of actin assembly at the leading edge/membrane protrusion and overall migration in Pfn1-deficient cells. These findings taken together with additional evidence of Lpd's and Ena/VASP's involvement in the hypermotile response of R88L-Pfn1 expresser are supportive of Pfn1's negative regulation of breast cancer cell motility through Lpd and in turn modulating Ena/VASP function at the leading edge. Whether Lpd has an additional contribution to the hypermotile response of Pfn1-knockdown cells in an Ena/VASP–independent manner is not clear at this point.

An interesting finding of the present study is the differential sensitivity of control vs Pfn1 knockdown MDA-231 cells to Lpd depletion. We showed that even though Lpd suppression alone can reduce the overall flare of protrusion in MDA-231 cells, this phenotype is rescued when cells are seeded on collagen-coated substrate and therefore, it is not surprising that Lpd knockdown does not have any significant impact on the overall motility of MDA-231 cells assessed on collagen-coated substrate. Pfn1-deficient deficient cells show a more severe phenotype in terms of lamellipodia formation and motility when subjected to Lpd depletion. Although the underlying reason is not clear, one possibility is that Lpd deficiency can be

compensated by RIAM-1 (Rap-interacting adaptor molecule), a Lpd-homolog that also binds to membrane PPI, Pfn1 and Ena/VASP proteins like Lpd [Lafuente et al., 2004]. Given that RIAM-1 regulates cell adhesion/spreading through actin organization and integrin activation, compensatory action of RIAM-1 might be more pronounced on adhesion promoting substrate such as on collage-coated tissue-culture substrate as used in our motility experiments. If RIAM-induced actin organization at the leading edge, at least, partially requires the involvement of Pfn1, cells lacking Pfn1 would also be expected to be hypersensitive to Lpd depletion as seen in our study. This will need to be investigated in the future.

Finally, we here report a novel finding that loss of Pfn1 expression enhances $PI(3,4)P_2$ presentation at the leading edge which clearly provides at least one mechanistic explanation for how Pfn1 could regulate Lpd distribution at the leading edge. Since Pfn1 can also bind to $PI(3,4)P_2$, one cannot absolutely rule out an additional possibility that potential competition between Pfn1 and Lpd for $PI(3,4)P_2$ binding could also be relieved upon loss of Pfn1 expression thereby further favoring Lpd targeting to the membrane. How might loss of Pfn1 enhance $PI(3,4)P_2$ accumulation at the leading edge? Given that $PI(3,4)P_2$ is predominantly generated by dephosphorylation of $PI(3,4)P_2$ by SHIP2 and we here show that Pfn1 depletion does not alter the activation of EGFR and AKT (a $PI(3,4,5)P_3$-directed event at the downstream of activated EGFR), one interesting possibility is that Pfn1's binding to $PI(3,4,5)P_3$ somehow sterically blocks SHIP2's access to $PI(3,4,5)P_3$ and hence prevents $PI(3,4,5)P_3$'s turnover to $PI(3,4)P_2$. This is not completely unreasonable since $PI(4,5)P_2$ hydrolysis by PLCγ (phospholipase-Cγ) has been previously shown to be inhibited by PPI-interaction of Pfn1, at least, in vitro [Sohn et al., 1995; Goldschmidt-Clermont et al., 1990]. Our future studies revealing how perturbation of Pfn1

affects the different PPI turnover pathways in response to RTK activation will provide further mechanistic insights into these biochemical events.

6.0 CONCLUSIONS

This work leads to a new paradigm of motility regulation by cytoskeletal molecules with pluri-ligand docking sites involving signaling cascade at the membrane. We have shown that this is how Pfn1, a generally considered pro-migratory molecule, can also inhibit cell motility by altering docking of other proteins at the membrane-cytosol interface, and this action is modulated by phospholipid interaction of Pfn1. The model we propose is in contrast to conventionally presented Pfn1's role in cell motility primarily through its actin and polyproline interactions. Based on this study, an intriguing hypothesis could be that Pfn1 affects cell migration through two pathways: **a traditional pro-migratory pathway** involving its direct action on actin polymerization at the leading edge through its actin and polyproline interactions, and **an anti-migratory pathway** involving suppression of $PI(3,4)P_2$-dependent leading edge targeting of pro-migratory complexes such as Lpd/VASP which is strictly regulated by PPI interaction of Pfn1. It is the relative contribution of these two opposing pathways which would ultimately define whether Pfn1 promotes or limits cell migration. Since the molecular environment of various PPI may vary from cell-type to cell-type, Pfn1-dependent modulation of cell motility through its PPI interaction could explain its context-dependent role in cell motility.

6.1 FUTURE DIRECTIONS

6.1.1. To investigate whether Lpd/VASP plays a role in breast cancer metastasis when Pfn1 expression is attenuated

Previous in vivo study from our laboratory demonstrate that overexpressing Pfn1 expression inhibits micro-metastasis of MDA-231 breast cancer cells in nude mice [Zou et al., 2007]; however, this study did not provide mechanistic insights on how Pfn1 overexpression limits migration and invasion of breast cancer cells in vivo. Recent in vitro studies show that overexpression of Pfn1 significantly suppresses breast cancer cell migration; conversely, limiting Pfn1 expression results in enhanced motility of MDA-231 breast cancer cells [Roy et al., 2004; Zou et al., 2007; Bae et al., 2009]. My previous in vitro studies further reveal that significantly increased motility of Pfn1-depleted MDA-231 breast cancer cells is through membrane targeting of Lpd/VASP complex at the protruding leading edge [Bae et al., 2009] suggesting that Lpd/VASP complex at the leading edge plays a role in membrane dynamics and overall breast cancer cell migration. However, whether the lamellipodial targeting of the Lpd/VASP complex can modulate the hyperinvasiveness (hypermetastasis) of MDA-231 breast cancer cells in vivo has not yet been investigated. Since surrounding microenvironment of tissue or matrix in vivo has an important factor on tumor cell invasion, I would like to extend my in vitro system to in vivo animal experiments.

To determine the importance of Lpd/VASP complex in metastatic ability of Pfn1-depleted MDA-231 cells on tumor metastasis, xenograft experiments will be performed with Pfn1 knockdown cells with or without co-suppression of Lpd or co-expression Ena/VASP mistargeting construct. Based on previous motility data, I expect that inhibiting Lpd/VASP

function should dramatically reduce metastasis of Pfn1-depleted MDA-231 cells. If true, perturbing Pfn1 and Lpd/VASP expression levels could prove to be a good molecular strategy for limiting metastasis of breast cancer cells.

6.1.2 To determine whether Pfn1 regulates the overall turnover and spatiotemporal dynamics of PPIs in breast cancer cells

Pfn1's interaction with membrane PPIs has mostly been confirmed in vitro and among the different PPIs, Pfn1 has been found to bind to $PI(4,5)P_2$, PIP_3, and $PI(3,4)P_2$ [Lu et al., 1996]. Biochemical experiments with purified constituents initially demonstrated that Pfn1 inhibits PLC-mediated $PI(4,5)P_2$ hydrolysis to IP3. Since these experiments were performed with purified constituents, determining whether Pfn1 influences PPI metabolism and the functional significance of such metabolism has not yet been thoroughly investigated in a cellular context. Based on recent observations from our laboratory demonstrating that limiting Pfn1 expression dramatically increases leading edge localization of $PI(3,4)P_2$ [unpublished data] and overexpressing Pfn1 significantly reduces PIP_3 generation in breast cancer cells [Das et al., 2009], I propose that Pfn1 plays a important role in regulating PPI turnover and consequently PPI-dependent downstream signaling.

To test this working model, I will first determine whether perturbing Pfn1 expression alters PPI turnover and the resulting products in MDA-231 breast cancer cells either in a basal or an EGF (or PDGF)-stimulated state by immunostaining and TLC-based detection assays. The next goal would be a fluorescence-based reporter assay or FRET-based (fluorescence resonance energy transfer) assay in real time to visualize the spatiotemporal dynamics of various PPIs at the cell membrane in response to growth factor (EGF, PEGF) stimulation in breast cancer cells. Overall,

this study will provide mechanistic insights as to whether and how perturbation of Pfn1 influences the different PPI turnover pathways and dynamics in response to receptor tyrosine kinase activation in cells.

BIBLIOGRAPHY

Allen P. (2003). Actin filament uncapping localizes to ruffling lamellae and rocketing vesicles. *Nat Cell Biol* **5**: 972-979.

Bae YH, **Johnson PA**, **Florek CA**, **Kohn J**, **Moghe PV**. (2006). Minute changes in composition of polymer substrates produce amplified differences in cell adhesion and motility via optimal ligand conditioning. *Acta Biomater* **2**: 473-482

Bae YH, Ding Z, Zou L, Wells A, Gertler F, Roy P. (2009). Loss of profilin-1 expression enhances breast cancer cell motility by Ena/VASP proteins. *J Cell Physiol* **219**: 354-364.

Barzik M, Kotova TI, Higgs HN, Hazelwood L, Hanein D, Gertler FB, Schafer DA. (2005). Ena/VASP proteins enhance actin polymerization in the presence of barbed end capping proteins. *J Biol Chem* **280**: 28653-28662.

Bear JE, Loureiro JJ, Libova I, Fassler R, Wehland J, Gertler FB. (2000). Negative regulation of fibroblast motility by Ena/VASP proteins. *Cell* **101**: 717-728.

Bear JE, Svitkina TM, Krause M, Schafer DA, Loureiro JJ, Strasser GA, Maly IV, Chaga OY, Cooper JA, Borisy GG, Gertler FB. (2002). Antagonism between Ena/VASP proteins and actin filament capping regulates fibroblast motility. *Cell* **109**: 509-521.

Blume-Jensen P, Hunter T. (2001). Oncogenic kinase signalling. *Nature* **411**: 355-65.

Bottcher RT, Wiesner S, Braun A, Wimmer R, Berna A, Elad N, Medalia O, Pfeifer A, Aszodi A, Costell M. (2009). Profilin 1 is required for abscission during late cytokinesis of chondrocytes. *Embo J.* **28**: 1157-1169.

Bubb MR, Yarmola EG, Gibson BG, Southwick FS. (2003). Depolymerization of actin filaments by profilin: Effects of profilin on capping protein function. *J Biol Chem* **278**: 24629-24635.

Cantley LC, Neel BG. (1999). New insights into tumor suppression: PTEN suppresses tumor formation by restraining the phosphoinositide 3-kinase/AKT pathway. *Proc Natl Acad Sci U S A* **96**: 4240-4245.

Cenni V, Sirri A, Riccio M, Lattanzi G, Santi S, de Pol A, Maraldi NM, Marmiroli S. (2003). Targeting of the Akt/PKB kinase to the actin skeleton. *Cell Mol Life Sci* **60**: 2710-2720.

Chan AY, Bailly M, Zebda N, Segall JE, Condeelis JS. (2000). Role of cofilin in epidermal growth factor-stimulated actin polymerization and lamellipod protrusion. *J Cell Biol* **148**: 531-542.

Chaudhary A *et al*. (1998). Probing the phosphoinositide 4,5-bisphosphate binding site of human profilin I. *Chem Biol* **5**: 273-281.

Chen P, Murphy-Ullrich J, Wells A. (1996). A role for gelsolin in actuating epidermal growth factor receptor-mediated cell motility. *J Cell Biol* **134**: 689-698.

Chiang AC, Massagué J. (2008). Molecular Basis of Metastasis. *N Engl J Med* **359**: 2814-2823.

Clark EA, Golub TR, Lander S, Hynes RO. (2000). Genomic analysis of metastasis reveals an essential role of RhoC. *Nature* **406**: 532-535.

Das T, Bae YH, Wells A, Roy P. (2009). Profilin-1 overexpression upregulates PTEN and suppresses AKT activation in breast cancer cells. *J Cell Physiol* **218**: 436-443.

Diakonova M, Bokoch G, and Swanson JA. (2002). Dynamics of cytoskeletal proteins during Fcgamma receptor-mediated phagocytosis in macrophages. *Mol Biol Cell* **13**(2): 402-411.

Ding Z, Lambrechts A, Parepally M, Roy P. (2006). Silencing profilin-1 inhibits endothelial cell proliferation, migration and cord morphogenesis. *J Cell Sci* **119**: 4127-4137.

Ding Z, Gau D, Deasy B, Wells, A, Roy P. (2009). Both actin and polyproline interactions of Profilin-1 are required for migration, invasion and capillary morphogenesis of vascular endothelial cells. *Exp Cell Res* **315**: 2963-2973.

Engers R, Gabbert HE. (2000). Mechanisms of tumor metastasis: cell biological aspects and clinical implications. *J Cancer Res Clin Oncol* **126**: 682-692.

Ezezika OC, Younger NS, Lu J, Kaiser DA, Corbin ZA, Nolen BJ, Kovar DR, Pollard TD. (2009). Incompatibility with formin Cdc12p prevents human profilin from substituting for fission yeast profilin: insights from crystal structures of fission yeast profilin. *J Biol Chem* **284**: 2088-2097.

Fedorov AA *et al*. (1994). X-ray structures of isoforms of the actin-binding protein profilin that differ in their affinity for phosphatidylinositol phosphates. *Proc Natl Acad Sci U S A* **91**: 8636-8640.

Feldner J, Brandt B. (2002). Cancer cell motility--on the road from c-erbB-2 receptor steered signaling to actin reorganization. *Exp Cell Res* **272**: 93-108.

Ferron F, Rebowski G, Lee SH, Dominguez R. (2007). Structural basis for the recruitment of profilin-actin complexes during filament elongation by Ena/VASP. *EMBO J* **26**: 4597-4606.

Geese M, Loureiro JJ, Bear JE, Wehland J, Gertler FB, Sechi AS. (2002). Contribution of Ena/VASP proteins to intracellular motility of listeria requires phosphorylation and proline-rich core but not F-actin binding or multimerization. *Mol Biol Cell* **13**: 2383-2396.

Geraghty KM, Chen S, Harthill JE, Ibrahim AF, Toth R, Morrice NA, Vandermoere F, Moorhead GB, Hardie DG, MacKintosh C. (2007). Regulation of multisite phosphorylation and 14-3-3 binding of AS160 in response to IGF-1, EGF, PMA and AICAR. *Biochem J*. **407**: 231-241.

Giesemann T, Rathke-Hartlieb S, Rothkegel M, Bartsch JW, Buchmeier S, Jockusch BM, Jockusch H. (1999). A role for polyproline motifs in the spinal muscular atrophy protein SMN. Profilins bind to and colocalize with smn in nuclear gems. *J Biol Chem* **274**: 37908-37914.

Goldschmidt-Clermont PJ, Machesky LM, Baldassare JJ, Pollard TD. (1990). The actin-binding protein profilin binds to PIP2 and inhibits its hydrolysis by phospholipase C. *Science* **247**: 1575-1578.

Goldschmidt-Clermont PJ *et al*. (1991). Regulation of phospholipase C-gamma 1 by profilin and tyrosine phosphorylation. *Science* **251**: 1231-1233.

Goswami S *et al*. (2005). Macrophages promote the invasion of breast carcinoma cells via a colony-stimulating factor-1/epidermal growth factor paracrine loop. *Cancer Res* **65**(12): 5278-5283.

Gronborg M, Kristiansen TZ, Iwahori A, Chang R, Reddy R, Sato N, Molina H, Jensen ON, Hruban RH, Goggins MG, Maitra A, Pandey A. (2006). Biomarker discovery from pancreatic cancer secretome using a differential proteomic approach. *Mol Cell Proteomics* **5**: 157-171.

Hartwig JH, Chambers KA, Hopcia KL, Kwiatkowski DJ. (1989). Association of profilin with filament-free regions of human leukocyte and platelet membranes and reversible membrane binding during platelet activation. *J Cell Biol* **109**: 1571-1579.

Haugh JM, Codazzi F, Teruel M, Meyer T. (2000). Spatial sensing in fibroblasts mediated by 3' phosphoinositides. *J Cell Biol* **151**: 1269-1280.

Haugwitz M, Noegel AA, Karakesisoglou J, Schleicher M. (1994). Dictyostelium amoebae that lack G-actin-sequestering profilins show defects in F-actin content, cytokinesis, and development. *Cell* **79**: 303-314.

Holt MR, Koffer A. (2001). Cell motility: Proline-rich proteins promote protrusions. *Trends Cell Biol* **11**: 38-46.

Hu E *et al.* (2001). Molecular cloning and characterization of profilin-3: a novel cytoskeleton-associated gene expressed in rat kidney and testes. *Exp Nephrol* **9**: 265-274.

Irie HY, Pearline RV, Grueneberg D, Hsia M, Ravichandran P, Kothari N, Natesan S, Brugge JS. (2005). Distinct roles of Akt1 and Akt2 in regulating cell migration and epithelial-mesenchymal transition. *J Cell Biol* **171**: 1023-1034.

Janmey P. (1994). Phosphoinositides and calcium as regulators of cellular actin assembly and disassembly. *Annu Rev Physiol* **56**: 169-191.

Janke J, Schluter K, Jandrig B, Theile M, Kolble K, Arnold W, Grinstein E, Schwartz A, Estevez-Schwarz L, Schlag PM, Jockusch BM, Scherneck S. (2000). Suppression of tumorigeniciy in breast cancer cells by the microfilament protein profilin 1. *J Exp Med* **191**: 1675-1685.

Kang F, Laine RO, Bubb MR, Southwick FS, Purich DL. (1997). Profilin interacts with the Gly-Pro-Pro-Pro-Pro-Pro sequences of vasodilator-stimulated phosphoprotein (VASP): implications for actin-based Listeria motility. *Biochemistry* **36**: 8384-8392.

Kang F, Purich DL, Southwick FS. (1999). Profilin promotes barbed-end actin filament assembly without lowering the critical concentration. *J Cell Biol* **274**: 36963-36972.

Karlsson L, Nystrom LE, Sundkvist I, Markey F, Lindberg U. (1977). Actin polymerizability is influenced by profilin, a low molecular weight protein in non-muscle cells. *J Mol Biol* **115**: 465-483.

Krause M, Leslie JD, Stewart M, Lafuente EM, Valderrama F, Jagannathan R, Strasser GA, Rubinson DA, Liu H,Way M, Yaffe MB, Boussiotis VA, Gertler FB. (2004). Lamellipodin, an Ena/VASP ligand, is implicated in the regulation of lamellipodial dynamics. *Dev Cell* **7**: 571-583.

Lacayo CI, Pincus Z, VanDuijn MM, Wilson CA, Fletcher DA, Gertler FB, Mogilner A, Theriot JA. (2007). Emergence of large-scale cell morphology and movement from local actin filament growth dynamics. *PLoS Biol* **5**: e233.

Lambrechts A, Braun A, Jonckheere V, Aszodi A, Lanier LM, Robbens J, Colen IV, Vandekerckhove J, Fassler R, Ampe C. (2000). Profilin II is alternatively spliced, resulting in profilin isoforms that are differently expressed and hae distinct biochemical properties. *Mol Cell Biol* **20**: 8209-8219.

Lambrechts A, Troys M, Ampe C. (2004). The actin cytoskeleton in normal and pathological cell motility. *IJBCB* 36: 1890-1909.

Lambrechts A, Jonckheere V, Peleman C, Polet D, De Vos W, Vandekerckhove J, Ampe C. (2006). Profilin-I-ligand interactions influence various aspects of neuronal differentiation. *J Cell Sci* **119**: 1570-1578.

Lassing I, Lindberg U. (1985). Specific interaction between PI(4,5)P_2 and profilactin. *Nature* **314**: 472-474.

Lassing I, Lindberg U. (1998). Specificity of the interaction between phosphatidylinositol 4,5-bisphosphate and the profilin:actin complex. *J Cell Biochem* **37**: 255-267.

Lauffenburger D, Horwitz A. (1996). Cell migration: a physically integrated molecular process. *Cell* **84**: 359-369.

Laurent V, Loisel TP, Harbeck B, Wehman A, Grobe L, Jockusch BM, Wehland J, Gertler FB, Carlier MF. (1999). Role of proteins of the Ena/VASP family in actin-based motility of Listeria monocytogenes. *J Cell Biol* **144**: 1245-1258.

Liu W, **Bagaitkar J**, **Watabe K**. (2007). **Roles of AKT signal in breast cancer.** *Front Biosci* **12**: 4011-4009.

Loisel TP, Boujemaa R, Pantaloni D, Carlier MF. (1999). Reconstitution of actin-based motility of Listeria and Shigella using pure proteins. *Nature* **401**: 613-616.

Loureiro JJ, Rubinson DA, Bear JE, Baltus GA, Kwiatkowski AV, Gertler FB. (2002). Critical roles of phosphorylation and actin binding motifs, but not the central proline-rich region, for Ena/vasodilator-stimulated phosphoprotein (VASP) function during cellmigration. *Mol Biol Cell* **13**: 2533-2546.

Lu J, Pollard TD. (2001). Profilin binding to poly-L-proline and actin monomers along with ability to catalyze actin nucleotide exchange is required for viability of fission yeast. *Mol Biol Cell* **12**: 1161-1175.

Lu PJ, Shieh WR, Rhee SG, Yin HL, Chen CS. (1996). Lipid products of phosphoinositide 3-kinase bind human profilin with high affinity. *Biochemistry* **35**: 14027-14034.

Machesky LM, Poland TD. (1993). Profilin as a potential mediator of membrane-cytoskeleton communication. *Trends Cell Biol* **3**: 381-385.

Mahoney NM *et al*. (1999). Profilin binds proline-rich ligands in two distinct amide backbone orientations. *Nat Struct Biol* **6**: 666-671.

Metzler WJ *et al*. (1994). Identification of the poly-L-proline-binding site on human profilin. *J Biol Chem* **269**: 4620-4625.

Miki H, Suetsugu S, Takenawa T. (1998). WAVE, a novel WASP-family protein involved in actin reorganization induced by Rac. *EMBO J* **17**: 6932-6941.

Mimuro H, Suzuki T, Suetsugu S, Miki H, Takenawa T, Sasakawa C. (2000). Profilin is required for sustaining efficient intra- and intercellular spreading of Shigella Flexneri. *J Biol Chem* **275**: 28893-28901.

Moens PD, Bagatolli LA. (2007). Profilin binding to sub-micellar concentrations of phosphatidylinositol (4,5) bisphosphate and phosphatidylinositol (3,4,5) trisphosphate. *Biochim Biophys Acta* **1768**: 439-449.

Nikolopoulos SN, Spengler BA, Kisselbach K, Evans AE, Biedler JL, Ross RA. (2000). The human non-muscle a-actinin protein encoded by the ACTN4 gene suppresses tumorigenicity of human neuroblastoma cells. *Oncogene* **19**: 380-386.

Obermann H *et al.* (2005). Novel testis-expressed profilin IV associated with acrosome biogenesis and spermatid elongation. *Mol Hum Reprod* **11**: 53-64.

Osaki M, Oshimura M, Ito H. (2004). PI3K-Akt pathway: its functions and alterations in human cancer. *Apoptosis* **9**: 667-676.

Panetti TS, **Hannah DF**, **Avraamides C**, **Gaughan JP**, **Marcinkiewicz C**, **Huttenlocher A**, **Mosher DF**. (2004). Extracellular matrix molecules regulate endothelial cell migration stimulated by lysophosphatidic acid. *J Thromb Haemost* **2**: 1645-1656.

Pantaloni D, Carlier MF. (1993). How profilin promotes actin filament assembly in the presence of thymosin beta-4. *Cell* **75**: 1007-1014.

Pasic L, Kotova T, Schafer DA. (2008). Ena/VASP proteins capture actin filament barbed ends. *J Biol Chem* **283**: 9814-9819.

Pawlak G, Helfman DM. (2001). Cytoskeletal changes in cell transformation and tumorigenesis. *Curr Opin Genet Dev* **11**: 41-47.

Petersen OW, Nielsen HL, Gudjonsson T, Villadsen R, Rank F, Niebuhr E, Bissell MJ, Rønnov-Jessen L. (2003). Epithelial to mesenchymal transition in human breast cancer can provide a nonmalignant stroma. *Am J Pathol* **162**: 391-402.

Philippar U, Roussos ET, Oser M, Yamaguchi H, Kim HD, Giampieri S, Wang Y, Goswami S, Wyckoff JB, Lauffenburger DA, Sahai E, Condeelis JS, Gertler FB. (2008). A mena invasion isoform potentiates EGF-induced carcinoma cell invasion and metastasis. *Dev Cell* **15**: 813-828.

Pollard TD, Borisy GG. (2003). Cellular motility driven by assembly and disassembly of actin filaments. *Cell* **112**: 453-465.

van Rheenen J, Song X, van Roosmalen W, Cammer M, Chen X, Desmarais V, Yip SC, Backer JM, Eddy RJ, Condeelis JS. (2007). EGF-induced PIP2 hydrolysis releases and

activates cofilin locally in carcinoma cells. *J Cell Biol* **179**: 1247-1259.

Richer SM, Stewart NK, Tomaszewski JW, Stone MJ, Oakley MG. (2008). NMR investigation of the binding between human profilin I and inositol 1,4,5-triphosphate, the soluble headgroup of phosphatidylinositol 4,5-bisphosphate. *Biochemistry* **47**(51): 13455-13462.

Ridley AJ, Schwartz MA, Burridge K, Firtel RA, Ginsberg MH, Borisy G, Parsons JT, Horwitz AR. (2003). Cell migration: integrating signals from front to back. *Science* **302**: 1704-1709.

Rottner K, Behrendt B, Small JV, Wehland J. (1999). VASP dynamics during lamellipodia protrusion. *Nat Cell Biol* **1**:321–322.

Rottman JB. (1999). Key role of chemokines and chemokine receptors in inflammation, immunity, neoplasia, and infectious disease. *Vet Pathol* **36**: 357-367.

Roy P, Jacobson K. (2004). Overexpression of profilin reduces the migration of invasive breast cancer cells. *Cell Motil Cytoskeleton* **57**: 84-95.

Roy P, Jaramillo M, Bae YH, Das T. (2008). Actin cytoskeleton and cancer. In The motile actin system in health and disease. (C. Ampe and A. Lambrechts, eds.) *Research Signpost* 93-122

Sainsbury R. (2000). Towards appropriate local surgery for patients with breast cancer. *Lancet* **356**: 1124-1125.

Schluter K, Jockusch BM, Rothkegel M. (1997). Profilin as regulators of actin dynamics. *Biochim Biophys Acta* **1359**: 97-109.

Schneider BP, Miller KD. (2005). Angiogenesis of breast cancer. *J Clin Oncol* **23**(8): 1782-1790.

Sheetz MP, Felsenfeld D, Galbraith CG, and Choquet D. (1999). Cell migration as a five-step cycle. *Biochem Soc Symp* **65**: 233-243.

Singh SS, Chauhan A, Murakami N, Chauhan VP. (1996). Profilin and gelsolin stimulate phosphatidylinositol 3-kinase activity. *Biochemistry* **35**: 16544-16549.

Skare P, Karlsson R. (2002). Evidence for two interaction regions for phosphatidylinositol (4,5)-bisphosphate on mammalian profilin I. *FEBS Lett* **522**: 119-124.

Smith K, Humphreys D, Hume PJ, Koronakis V. (2010). Enteropathogenic Escherichia coli recruits the cellular inositol phosphatase SHIP2 to regulate actin-pedestal formation. *Cell Host Microbe* **7**(1): 13-24.

Sohn RH, Chen J, Koblan KS, Bray PF, Goldschmidt-Clermont PJ. (1995). Localization of a binding site for phosphatidylinositol 4,5-bisphosphate on human profilin. *J Biol Chem* **270**: 21114-21120.

Suetsugu S, miki H, Takenawa T. (1998). The essential role of profilin in the assembly of actin for microspike formation. *EMBO J* **17**: 6516-6526.

Syriani E, Gomez-Cabrero A, Bosch M, Moya A, Abad E, Gual A, Gasull X, Morales M. (2008). Profilin induces lamellipodia by growth factor-independent mechanism. *FASEB J* **22**: 1581-1596.

Tanaka M, Mullaur L, Ogiso Y, Fujita H, Moriya S, Furuuchi K, Harabayashi T, Shinohara N, Koyanagi T, Kuzumaki N. (1995). Gelsolin: A candidate for suppressor of human bladder cancer. *Cancer Res* **55**: 3228-3232.

Theriot JA, Mitchison TJ. (1993). The three faces of profilin. *Cell* **75**(5): 835-838.

Theriot JA, Rosenblatt J, Portnoy DA, Goldschmidt-Clermont PJ, Mitchison TJ. (1994). Involvement of profilin in the actin-based motility of L. monocytogenes in cells and in cell-free extracts. *Cell* **76**: 505-517.

Velarde, N., Gunsalus, K. C. and Piano, F. (2007). Diverse roles of actin in C. elegans early embryogenesis. *BMC Dev Biol* **7**, 142.

Verheyen EM, Cooley L. (1994). Profilin mutations disrupt multiple actin-dependent processes during drosophila development. *Development* **120**: 717-728.

Wang FL,Wang Y, Wong WK, Liu Y, Addivinola J, Liang P, Chen LB, Kantoff PW, Pardee AB. (1996). Two differentially expressed genes in normal human prostate tissue and in carcinoma. *Cancer Res* **56**: 3634-3637.

Watanabe N *et al*. (1997). p140mDia, a mammalian homolog of Drosophila diaphanous, is a target protein for Rho small GTPase and is a ligand for profilin. *EMBO J* **16**: 3044-3056.

Welch DR, Steeg PS, Rinker-Schaeffer CW. (2000). Molecular biology of breast cancer metastasis: Genetic regulation of human breasty cancer metastasis. *Breast Cancer Res* **2**: 408-416.

Wills Z, Marr L, Zinn K, Goodman CS, Van Vactor D. (1999). Profilin and the Abl tyrosine kinase are required for motor axon outgrowth in the Drosophila embryo. *Neuron* **22**: 291-299.

Witke W, Podtelejnikov AV, Di Nardo A, Sutherland JD, Gurniak CB, Dotti C, Mann M. (1998). In mouse brain profilin I and profilin II associate with regulators of the endocytic pathway and actin assembly. *EMBO J* **17**: 967-976.

Witke W. (2004). The role of profilin complexes in cell motility and other cellular processes. *Trends Cell Biol* **14**: 461-469.

Wittenmayer N, Jandrig B, Rothkegel M, Schluter K, Arnold W, Haensch W, Scherneck S, Jockusch BM. (2004). Tumor suppressor activity of profilin requires a functional actin binding site. *Mol Biol Cell* **15**: 1600-1608.

Wittenmayer N, Rothkegel M, Jockusch BM, Schluter K. (2000). Functional characterization of green fluorescent protein-profilin fusion proteins. *Eur J Biochem* **267**: 5247-5256.

Wu N, Zhang W, Yang Y, Liang YL, Wang LY, Jin JW, Cai XM, Zha XL. (2006). Profilin-1 obtained by proteomic analysis in all-trans retinoic acid-treated hepatocarcinoma cell lines is involved in inhibition of cell proliferation and migration. *Proteomics* **6**: 6095-6106.

Wyckoff JB, Jones JG, Condeelis JS, Segall JE. (2000). A critical step in metastasis: in vivo analysis of intravasation at the primary tumor. *Cancer Res* **60**: 2504-2511.

Wyckoff JB *et al*. (2004). A paracrine loop between tumor cells and macrophages is required for tumor cell migration in mammary tumors. *Cancer Res* **64**(19): 7022-7029.

Xue C *et al*. (2006). Epidermal growth factor receptor overexpression results in increased tumor cell motility in vivo coordinately with enhanced intravasation and metastasis. *Cancer Res* **66**(1): 192-197.

Yamaguchi H, Wyckoff J, Condeelis J. (2005). Cell migration in tumors. *Curr Opin Cell Biol* **17**: 559-564.

Yip SC, Eddy RJ, Branch AM, Pang H, Wu H, Yan Y, Drees BE, Neilsen PO, Condeelis J, Backer JM. (2009). Quantification of PtdIns(3,4,5)P(3) dynamics in EGF-stimulated carcinoma cells: a comparison of PH-domain-mediated methods with immunological methods. *Biochem J*. **411**(2): 441-448.

Zou L, Hazan R, Roy P. (2009). Profilin-1 overexpression restores adherence junctions in MDA-MB-231 breast cancer cells in R-cadherin-dependent manner. *Cell Motil Cytoskeleton*. **66**(12):1048-1056.

Zou L, Jaramillo M, Whaley D, Wells A, Panchapakesa V, Das T, Roy P. (2007). Profilin-1 is a negative regulator of mammary carcinoma aggressiveness. *Br J Cancer* **97**: 1361-1371.